DOKUZ EYLÜL UNIVERSITY

GRADUATE SCHOOL OF NATURAL AND APPLIED SCIENCES

CABIN SUSPENSION SYSTEM DESIGN OF AN 8x8 WHEELED TACTICAL VEHICLE

by

Enis GÖGEN

August, 2014

İZMİR

CABIN SUSPENSION SYSTEM DESIGN OF AN 8x8 WHEELED TACTICAL VEHICLE

A Thesis Submitted to the
Graduate School of Natural and Applied Sciences of Dokuz Eylül University
In Partial Fulfillment of the Requirements for the Degree of Master of Science
in Mechanical Engineering, Machine Theory and Dynamics Program

by

Enis GÖGEN

August, 2014

İZMİR

M.Sc THESIS EXAMINATION RESULT FORM

We have read the thesis entitled **"CABIN SUSPENSION SYSTEM DESIGN OF A 8x8 WHEELED TACTICAL VEHICLE"** completed by **ENİS GÖGEN** under supervision of **ASSOC. PROF. LEVENT MALGACA** and we certify that in our opinion it is fully adequate, in scope and in quality, as a thesis for the degree of Master of Science.

Assoc. Prof. Levent MALGACA

Supervisor

ASSIST. PROF. Ayşe ALTAÇ

(Jury Member)

ASSIST. PROF. M. MURAT ZORAC

(Jury Member)

Prof.Dr. Ayşe OKUR
Director
Graduate School of Natural and Applied Sciences

ACKNOWLEDGEMENTS

I would like to thank my supervisor, Associate Professor Levent MALGACA for his support and guidance during all phases of this study.

I would also like to thank Msc Mechanical Engineer Mr. Sertaç AKTAŞ, who allowed and encouraged me to start master of science program, his support and advices have been greatly appreciated.

This study is dedicated to my beloved family, who always positively prod me by reminding the importance of completing this thesis study as worthy, and always keeping their faith on me.

Enis GÖGEN

CABIN SUSPENSION SYSTEM DESIGN OF AN 8x8 WHEELED TACTICAL VEHICLE

ABSTRACT

In this thesis study, cabin suspension system design is performed for a 44 ton gross vehicle weight, eight wheeler tactical vehicle equipped with four-point cabin suspension system, and dynamic responses are examined under various base excitations. During cabin suspension system design, full vehicle model is obtained because of the difficulties while calculating dynamic input forces transferred from base excitations.

Vehicle's three-dimensioned FE model is generated in ANSYS software. In FE model, driver, passengers and superstructure are defined as mass21, Spring-damper elements are defined as combin14, primary suspension double wishbone control arms are defined as rigid element mpc184, vehicle frame, cabin and cargobed are defined as shell63.

Axle loads are calculated by considering weight distribution via Ten-DOF half vehicle model, in order to specify spring-damper element coefficients of suspension systems. Coefficients of spring-damper elements between wheels-frame, and frame-cabin, respectively belongs to primary and secondary suspension systems are specified by calculating via these axle loads. Being aware for what kind of excitation occurs on vehicle according to different kind of base excitations, is important from dynamic analysis point of view. For that reason, vehicle's natural frequencies and mode shapes for each frequency are determined by modal analysis.. After modeling the base excitations by MATLAB, they were transformed to suitable format with respect to time via VisualBasic in order to be used in ANSYS. Obstacles represent step and sinusoidal base excitations.

Dynamic responses are obtained as displacement, velocity and acceleration. These responses obtained for different base excitations are examined from cabin and

passenger pitch, roll, yaw and bounce point of views. Vehicle frame responses are also examined in order to compare the damping level of vehicle's multibody motions. Conformity of calculated spring-damper coefficients for vehicle cabin suspension design is evaluated by comparing the obtained dynamic results.

Keywords : 8x8 vehicle, cabin suspension, dynamic analysis, finite elements

8x8 TEKERLEKLİ TAKTİK ARACIN KABİN SÜSPANSİYON SİSTEMİ TASARIMI

ÖZ

Bu tez çalışmasında, dört nokta kabin süspansiyon sistemi ile donatılmış 44 ton ağırlığında, sekiz tekerlekli bir taktik aracın kabin süspansiyon tasarımı yapılarak farklı yol girdileri altında dinamik cevapları incelenmiştir. Kabin süspansiyon sisteminin tasarımında, yol girdilerinden kabine aktarılan dinamik yüklerin hesaplanması güç olduğundan tam araç modeli ele alınmıştır.

Aracın üç boyutlu sonlu elemanlar modeli ANSYS programında kurulmuştur. Sonlu elemanlar modelinde, sürücü, yolcu ve üstyapı yükü mass21, yay-sönüm elamanları combin14, birincil süspansiyon alt ve üst salıncak kolları rijit eleman olan mpc184, araç şasisi, kabin, üstyapı taşıyıcı platform shell63 olarak tanımlanmıştır.

Süspansiyon sistemlerindeki yay-sönüm elemanlarının değerlerini belirlemek için 10 serbestlik dereceli yarım araç modelindeki ağırlık dağılımı dikkate alınarak dingil yükleri hesaplanmıştır. Modelde, birincil ve ikincil süspansiyon sistemlerindeki sırasıyla şasi-tekerlek ve şasi-kabin arasındaki yay-sönüm elemanlarının değerleri bu dingil yüklerine göre hesaplanarak tanımlanmıştır. Aracın dinamik yol girdilerine karşı hangi tip zorlamaya maruz kalacağının bilinmesi dinamik analiz açısından önemlidir. Bu nedenle modal analiz ile aracın doğal frekansları ve bu frekanslara karşılık gelen doğal titreşim biçimleri belirlenmiştir. Dinamik yol girdileri MATLAB programında modellendikten sonra Visual Basic ile zamana bağlı olarak ANSYS için uygun formata dönüştürülmüştür. Engeller, adım ve sinüzoidal yol şartlarını temsil eder.

Dinamik cevaplar, yer değiştirme, hız, ivme cinsinden elde edilmiştir. Farklı yol girdileri için elde edilen dinamik cevaplar, kabin ve yolcuların baş sallama, yalpalama ve zıplama reaksiyonları açısından incelenmiştir. Aracın çoklu kütle hareketlerinin sönüm seviyelerini karşılaştırmak maksadı ile araç şasisinin de

reaksiyonları irdelenmiştir. Aracın kabin süspansiyon tasarımında seçilen yay-sönüm sabitlerinin uygunluğu elde edilen dinamik cevaplar kıyaslanarak değerlendirilmiştir.

Anahtar kelimeler: 8x8 araç, kabin süspansiyonu, dinamik analiz, sonlu elemanlar.

CONTENTS

Page

LIST OF FIGURES

Page

LIST OF TABLES

Page

CHAPTER ONE
INTRODUCTION

1.1 Suspension Systems of Wheeled Tactical Vehicles

Wheeled tactical vehicles or in other words off-road vehicles can be equipped by both rigid and independent primary suspension systems. The primary function of a suspension system is to isolate the vehicle as far as practicable from shock loading and vibrations due to irregularities of the road surface (Sujatha & Tejesu, 2002). The choice of the system can be determined according to the usage, road conditions, payload and economic targets of the manufacturer.

The classic driven rigid axle, or so called 'live axle', is supported and located by two leaf springs (Dixon, 2009), and shock absorbers. Both parabolic and conventional type of leaf springs are in usage for wheeled tactical vehicles. When the axles are suspended to the vehicle frame with a coil spring or an air bellow, trailing arms and V-Links are also assembled to the system in order to meet the lateral and longitudinal reaction forces.

Most common type of independent suspension system used for wheeled tactical vehicles is double wishbone suspension system. It consists of upper and the lower wishbone arms pivoted to the frame member. The spring is placed in between the lower wishbone and the underside of the cross-member. A shock absorber is placed inside the coil spring is attached to the cross-member and to lower wishbone member. The wishbones not only position the wheels and transmit the vehicle load to the springs, but also resist acceleration, braking, and cornering forces (Jagirdar, Dadar & Sulakhe, 2010).

1.2 The Effect of Suspension System To Ride Comfort and Ride Safety

As it is referred in previous section, wheeled tactical vehicles can be equipped by both rigid and independent suspension systems. However strength of the system is

decided to be the main criteria, handling and ride comfort have the key roles during determining the vehicle's suspension system. Acceptable ride comfort limits vary according to the different conditions and also the type of the vehicle (Els, 2005). Apart from comfort criteria, the dynamic forces between road and tire should be taken into account in order to improve the vehicle handling and decrease the deterioration of the road surface (Vaculin & Valasek, 2005).

When designing a vehicle suspension system, it is well-known that spring and damper characteristics required for good handling of a vehicle are not the same as those required for good ride comfort. Any choice of spring and damper characteristics is therefore necessarily a compromise between ride comfort and handling (Els, Theron, Uys & Thoresson, 2007).

Military trucks, in general tend to use live axle suspension systems with rigid axles (Jagirdar et. al., 2010). A rigid axle suspension system is consist of rigid alive axles suspended by leaf springs, coil springs or even air bellows. Special precautions have to be taken in order to meet the vertical and lateral force reactions during the vehicle is going over an obstacle or even cornering with unusual accelerations. When the bouncy road conditions were considered for off-road conditions, engineers decided to generate the rigid axle suspension systems with soft springs in order to supply the smooth ride characteristic. By the way, the wheel contact with the surface will always be supplied. However, a smooth and comfortable ride occurred, handling and steering will be the main problem because of the suspension geometry. Because of right and left hand side wheels connection via rigid axle tube, wheels toe angle changes are inevitable during right and left hand side wheels asynchronous travels. How big the asynchronous travel distance is, toe angle changes are also big in this scope. The numerical and analytical results also show that with decreasing suspension system index, the ride comfort increases and handling becomes worse (Zehsaz, Tahami, Fasihi & Majidi, 2012).So engineers decided to generate the system with tougher springs in order to decrease the toe angle changes, but this cause a hard ride characteristic, and the comfort feeling is also affected negatively.

When designing vehicle suspensions, the dual objective is to minimize the vertical forces transmitted to the passenger, and to maximize the tire-to-road contact for handling and safety (Dowds & O'Dwyer, 2005). For stability and handling, more stiffer suspension is required whereas, for ride comfort comparatively soft suspension is suitable (Hussain, 2012), which is a design trade-off between ride quality and the stability of the vehicle (Daudpoto, Hussain & Memon, 2012).

In order to supply a both comfortable and safety ride, a system which allows soft springing and on the other hand a safety ride, is required to be generated. Engineers are decided, this will be done by letting the wheels travel independently. So a new design that will suspend the wheels independently on the vehicle frame is generated called independent suspension system. When a wheel goes over an obstacle, other wheel will not be affected, so this will have a positive effect on handling. On the other hand springing can be adjusted softer enough in order to supply a comfortable ride. With independent suspension, the wheels can move independently of each other, which reduce body movement (Maddaiah, Ratman, Kumar, K., Kumar, A., Yesu & Kumar, V., 2013).

1.3 The Necessity of Cabin Suspension

However lots of applications are performed on vehicle's primary suspension systems in order to decrease the roll and pitch motions of the vehicle, still the results are not declared to be flawless. Wheeled tactical vehicles are equipped with cabin suspension systems which are called secondary suspension systems. The main purpose of these systems is to minimize the vibrations transmitted to the driver (Maddaiah et. al., 2013). The cabin structure is located onto the vehicle frame by means of spring-damper elements. When the height of the vehicle cabin is taken into account, a few precautions have to be taken to keep the driver's ride height stable. As a result generating a cabin suspension system seems inevitable for off-road vehicles. For the design of secondary suspension, driving comfort and vehicle feedback are the most important criteria (Maurice & Vandenhoudt, 2013).

Multibody systems are composed of rigid bodies connected together with flexible connections providing additional (internal or shape) degrees of freedom to the system (Sanyal, 2004). Various examples demonstrate that connection type cannot be done rigid for the multibody dynamic systems that are assembled one on another which own different natural frequencies on same modes. Deformations occur during the fatigue life of subcomponents. So this can be accepted as another necessity for cabin suspension.

Seat ergonomics is also another issue that affects the ride comfort, directly. Since, it is a main part of the comfort phenomenon, seats in the vehicle cabin have also particular suspension systems that work as an isolator between the passengers and the cabin structure. Improving the ergonomics of the seat can lessen the adverse effects of vehicle vibration. Adding a secondary suspension mechanism to the driver's seat of heavy vehicles is another solution that was found to reduce the vibration induced by the seat (Valero, Amirouche, Mayton & Jobes, 2007).

1.4 Flow Chart of the Study

Flow chart defines the steps of this study, beginning from vehicle specification, until generating nodal reactions and vehicle dynamic responses as described in Figure1.1.

The study starts by presenting the vehicle's physical dimensions, which are necessary for further calculations for this study. A 10 DOF model will be build in order to calculate the axle loads in static position for the location of the payload at vehicle's maximum carrying capacity. Primary suspension system coefficients will be determined according to these calculated axle loads, and then secondary suspension system coefficients will be determined according to comfort criteria.

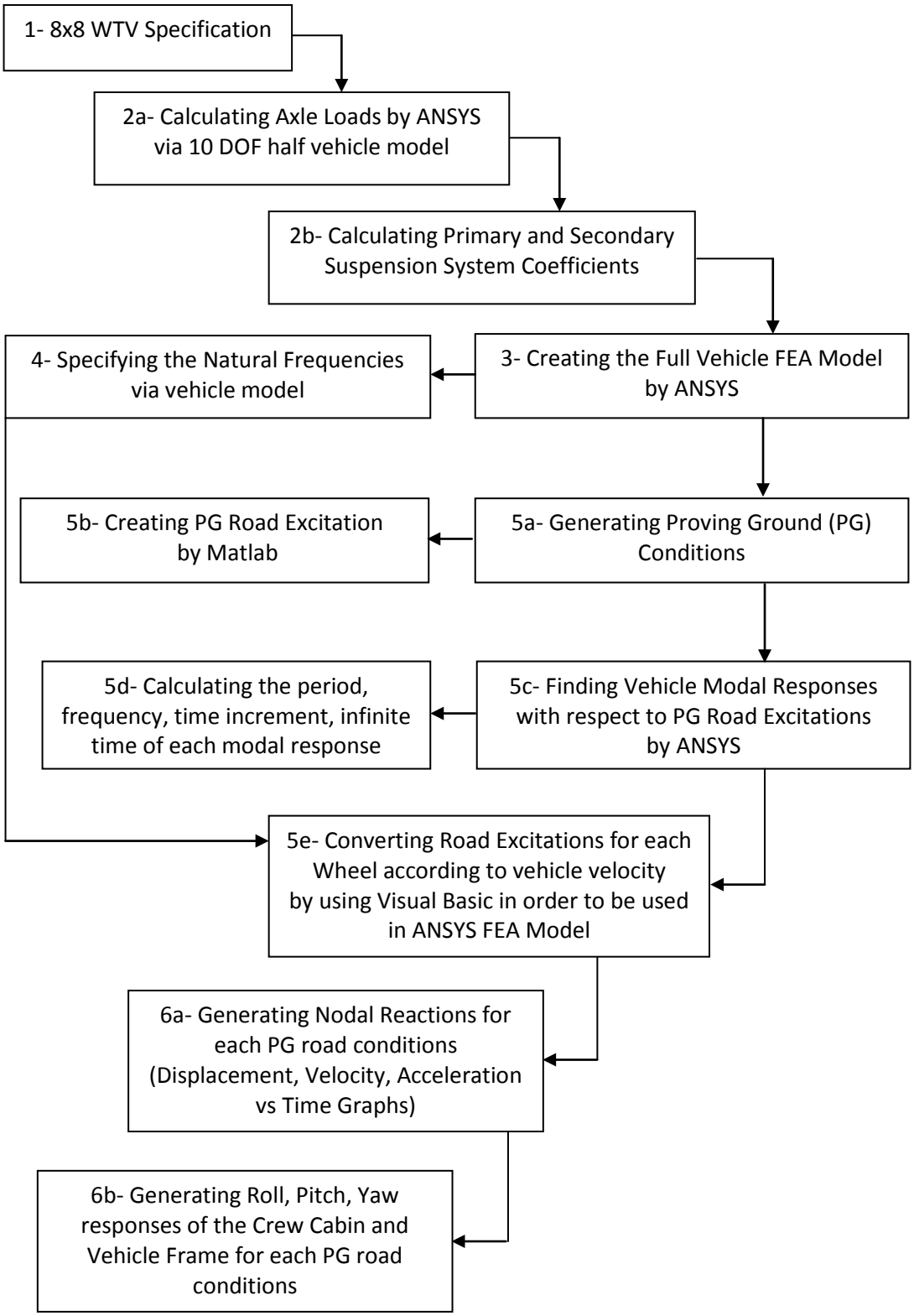

Figure 1.1 Flow chart of the study

Full vehicle FE model will be generated according to vehicle physical dimensions and calculated primary-secondary suspension system coefficients. Modal analysis will be performed and natural frequencies of the vehicle will be stated for each dynamic reactions. Vehicle is decided to be tested through a few road conditions. So these road conditions called "Proving Ground" in this paper will be generated. Vehicle modal responses will be stated thanks to these proving ground road excitations, and modal properties especially time increments will be calculated in order to be used as inputs during FE simulations. Using correct time increment value is important to excite the system on correct natural frequency mode. By nature of the dynamic fiction of this study, inputs should be prepared separately for each vehicle wheel, relative to vehicle speed. So different kind of softwares are used to prepare the relevant inputs for FE simulations. Matlab is used to define general proving ground road excitations, and Visual Basic is for setting the inputs separately for each wheel. Once the simulations run, nodal reactions as displacement, velocity and acceleration versus time results will be achieved. These results will give an idea for the bounce reaction of the vehicle. For other dynamic reactions such as roll, pitch and yaw responses, reaction responses will be calculated via formulas using nodal reactions used for bounce reactions.

CHAPTER TWO
8x8 WHEELED TACTICAL VEHICLE SPECIFICATION

This thesis examine a 44 ton gross vehicle weight 8x8 WTV equipped with double wishbone independent primary suspension systems for each wheels. Vehicle also has 4 point cabin suspension system to be evaluated as secondary suspension system. Both primary and secondary suspension elements are coil springs and hydraulic shock absorbers.

2.1 Vehicle Dimensions

Vehicle dimensions are given in Figure 2.1

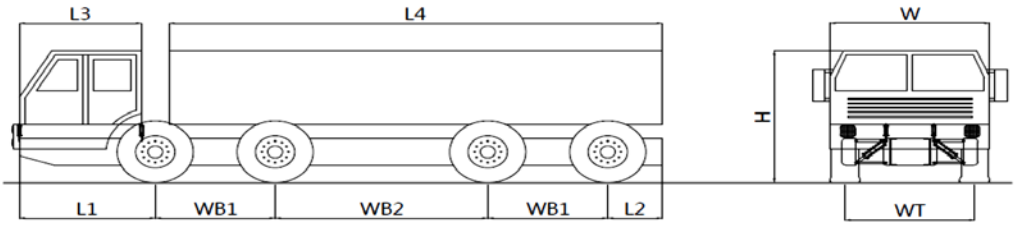

Figure 2.1 Vehicle views

Table 2.1 Vehicle dimensions

L1	Front Overhang	1995 mm
L2	Rear Overhang	1000 mm
L3	Crew Cabin Length	1745 mm
L4	Superstructure Length	9050 mm
WB1	First Wheelbase	2200 mm
WB2	Second Wheelbase	3900 mm
W	Vehicle Width	3070 mm
H	Crew Cabin Length	3000 mm
WT	Wheel Track	2375 mm

2.2 Weight Distribution

The free body diagram of the vehicle is configured as 10 DOF half vehicle model in ANSYS. Static forces are applied to the model.

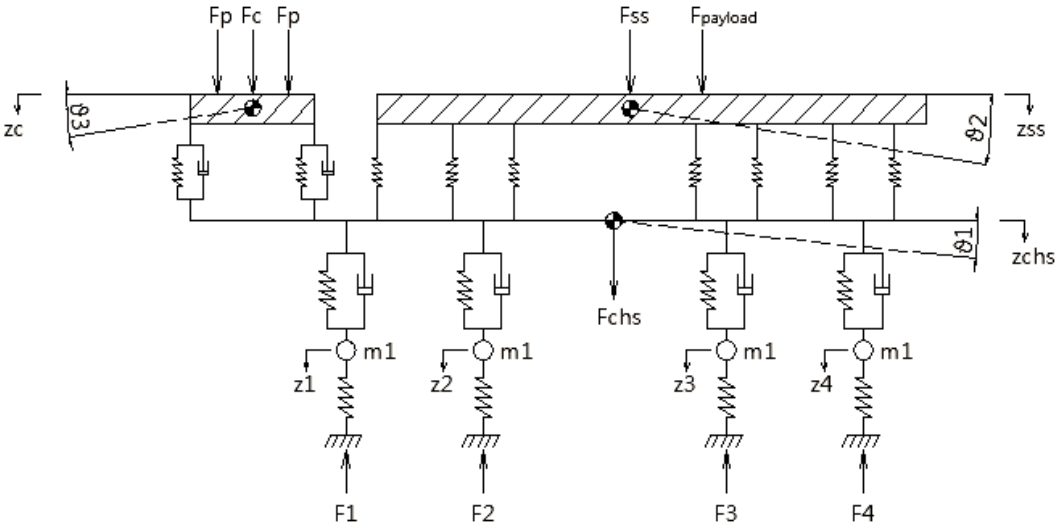

Figure 2.2 Free body diagram of the vehicle

Table 2.2 Vehicle weight table

Personnel Weight : 80 kg	Fp	2 x 80 x 9.81 = 1569.6 N
Crew Cabin Weight : 1700 kg	Fc	16677 N
Superstructure Weight : 5300 kg	Fss	51993 N
Payload : 18880 kg	Fpayload	185212.8 N
Chassis Weight : 13800 kg	Fchs	135378 N

By this layout each axle will carry equally 11000 kg. So the handling, comfort, ride height and even tire wears will be optimized. Also this layout shows the vehicle axles' maximum carrying capacity.

2.3 Specifying Spring-Damper Element Coefficients

2.3.1 Primary Suspension System Coefficient Calculation

System's first and second front axles natural frequencies will be adjusted to nearly 1 Hz which is accepted as an optimal comfort criteria for a fully laden vehicle. Third and fourth rear axles will be set by %20 harder according to front axles in order to control the pitch motion of the vehicle. Tire spring coefficient will be neglected during calculations. Final vertical natural frequency of the vehicle will be found by finite element model. A Double Wishbone suspension layout is shown in Figure 2.3, below. Conversion ratio (i) will be calculated according to parameters, below.

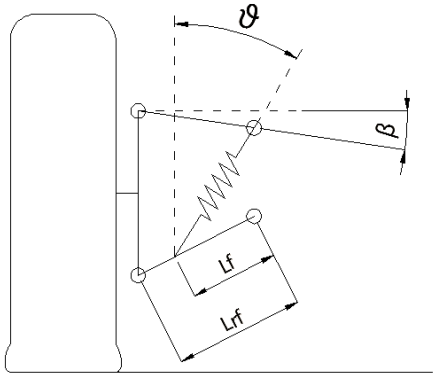

Figure 2.3 Double wishbone suspension layout

$$i = \frac{Lrf}{Lf} . \frac{1}{cos\theta.(1-tan\beta.tan\theta)} \tag{2.1}$$

Table 2.3 Coefficients

β	Upper Control Arm Angle to the Horizontal
ϑ	Spring-Damper Angle to the Vertical
Lrf	Lower Control Arm Length
Lf	Distance between spring-damper connection and Lower Control Arm joint

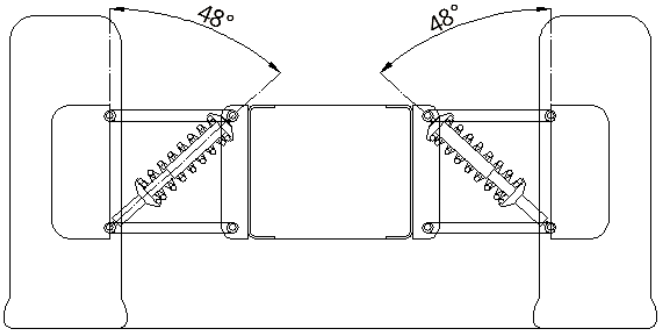

Figure 2.4 8x8 WTV suspension layout

As it is seen in Figure 2.4, vehicle's control arms are parallel to the ground on design position, means "β" is equal to zero. " ϑ" is 48° as it is specified on the figure, Lrf is equal to Lf. The conversion ratio will be ;

$$i = \frac{1}{1}.\frac{1}{cos48.(1-tan0.tan48)} = \frac{1}{cos48} = 1.494 \quad (2.2)$$

$$k_w = (2\pi f)^2.m_S \quad (2.3)$$

$$m_S = m_T - m_U \quad (2.4)$$

$$k = k_w.i^2 \quad (2.5)$$

Table 2.4 Unknowns of equations

k_W	Spring Coefficient reduced to wheel axis	TBC
k	Spring Coefficient	TBC
i	Conversion ratio	1.494
f_f	Front axles (1st and 2nd) frequency	1 Hz
f_r	Rear axles (3rd and 4th) frequency	1.2 Hz
m_T	Total mass per one wheel	5500 kg
m_S	Sprung mass per one wheel	5000 kg
m_U	Unsprung mass per one wheel	500 kg

For front axles f_f = 1 Hz ;

$$m_S = m_T - m_U = 5500 - 500 = 5000\ kg \quad (2.6)$$

$$k_W = (2\pi\ x\ 1)^2\ x\ 5000 = 197392\ N/m \quad (2.7)$$

$$k_f = k_W.i^2 = 197392\ x\ 1.494^2 = 440586.25\ N/m \quad (2.8)$$

For rear axles f_r = 1.2 Hz ;

$$k_W = (2\pi\ x\ 1.2)^2\ x\ 5000 = 284244.6\ N/m \quad (2.9)$$

$$k_r = k_W.i^2 = 284244.6\ x\ 1.494^2 = 634444.195\ N/m \quad (2.10)$$

For front shock absorbers (dampers) ;

$$D = \frac{c_W}{2.\sqrt{k_W.m_S}} \quad (2.11)$$

$$c = c_W.i^2 \quad (2.12)$$

where "D" is the system damping ratio, and " c_w " is shock absorber damping coefficient reduced to wheels, "c" is shock absorber damping coefficient.

For D=0.25 front shock absorber damping coefficient will be;

$$0.25 = \frac{c_{Wf}}{2.\sqrt{197392\ x\ 5000}} \quad (2.13)$$

$$c_{Wf} = 15707.96\ Ns/m \quad (2.14)$$

$$c_f = 15707.96\ x\ 1.494^2 = 35060.73\ Ns/m \quad (2.15)$$

Rear shock absorber damping coefficient will be;

$$0.25 = \frac{c_{Wr}}{2.\sqrt{284244.6\ x\ 5000}} \quad (2.16)$$

$$c_{Wr} = 18849.56\ Ns/m \quad (2.17)$$

$$c_r = 18849.56\ x\ 1.494^2 = 42072.88\ Ns/m \quad (2.18)$$

2.3.2 Secondary Suspension System Coefficient Calculation

For cabin suspension system which is secondary suspension system of the vehicle; the initial calculations will be performed as the crew cabin is equally suspended on the vehicle frame by 4 spring-damper elements. Secondary suspension system elements will be listed in below table. Frequency and damping ratios will be calculated according to these elements;

Table 2.5 Cabin suspension system unknowns

k_C	Cabin Spring Coefficient	16873.2 N/m
c_C	Cabin Shock Absorber Damping Ratio	1463.14 Ns/m
k_{PS}	Passenger Seat Spring Coefficient	3727.8 N/m
c_{PS}	Passenger Seat Shock Absorber Damping Ratio	2500 Ns/m
m_P	Passenger mass	80 kg
m_{CSD}	Sprung mass per one spring-damper element	425 kg
f_C	Cabin Frequency	TBC
D_C	Cabin Damping Ratio	TBC
f_P	Passenger Seat Frequency	TBC
D_P	Passenger Seat Damping Ratio	TBC

$$f_C = \frac{1}{2\pi}\sqrt{\frac{k_C}{m_{CSD}}} = \frac{1}{2\pi}\sqrt{\frac{16873.2}{425}} = 1 \text{ Hz} \quad (2.19)$$

$$D_C = \frac{c_C}{2\sqrt{k_C.m_{CSD}}} = \frac{1463.14}{2\sqrt{16873.2x425}} = 0.27 \quad (2.20)$$

$$f_P = \frac{1}{2\pi}\sqrt{\frac{k_{PS}}{m_P}} = \frac{1}{2\pi}\sqrt{\frac{3727.8}{80}} = 1.086\ Hz \quad (2.21)$$

$$D_P = \frac{c_{PS}}{2\sqrt{k_{PS}.m_P}} = \frac{250}{2\sqrt{3727.8x80}} = 0.23 \quad (2.22)$$

All frequency responses are set to nearly 1 Hz, as it is commonly known as an optimum comfort range for human body. Damping ratios are around 0.25 ± 0.2

2.3.3 Hardpoints of the Vehicle

According to the vehicle layout, attachment points including joints and connections of subcomponents of the suspension system called as hardpoints will be identified in order to make preliminary preparations for finite element modeling.

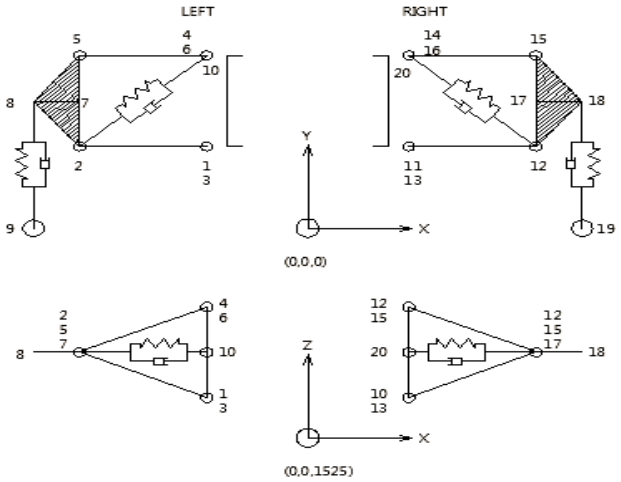

Figure 2.5 Frame and primary suspension system hardpoints

1st Axle		2nd Axle	
LEFT	RIGHT	LEFT	RIGHT
1- (1745,-437.5,450)	11- (1745,437.5,450)	21- (3945,-437.5,450)	31- (3945,437.5,450)
2- (1995,-987.5,450)	12- (1995,987.5,450)	22- (4195,-987.5,450)	32- (4195,987.5,450)
3- (2245,-437.5,450)	13- (2245,437.5,450)	23- (4445,-437.5,450)	33- (4445,437.5,450)
4- (1745,-437.5,950)	14- (1745,437.5,950)	24- (3945,-437.5,950)	34- (3945,437.5,950)
5- (1995,-987.5,950)	15- (1995,987.5,950)	25- (4195,-987.5,950)	35- (4195,987.5,950)
6- (2245,-437.5,950)	16- (2245,437.5,950)	26- (4445,-437.5,950)	36- (4445,437.5,950)
7- (1995,-987.5,700)	17- (1995,987.5,700)	27- (4195,-987.5,700)	37- (4195,987.5,700)
8- (1995,-1187.5,700)	18- (1995,1187.5,700)	28- (4195,-1187.5,700)	38- (4195,1187.5,700)
9- (1995,-1187.5,0)	19- (1995,1187.5,0)	29- (4195,-1187.5,0)	39- (4195,1187.5,0)
10- (1995,-437.5,950)	20- (1995,437.5,950)	30- (4195,-437.5,950)	40- (4195,437.5,950)

Figure 2.6 First and second axles hardpoints

3rd Axle		4th Axle	
LEFT	RIGHT	LEFT	RIGHT
41- (7845,-437.5,450)	51- (7845,437.5,450)	61- (10045,-437.5,450)	71- (10045,437.5,450)
42- (8095,-987.5,450)	52- (8095,987.5,450)	62- (10295,-987.5,450)	72- (10295,987.5,450)
43- (8345,-437.5,450)	53- (8345,437.5,450)	63- (10545,-437.5,450)	73- (10545,437.5,450)
44- (7845,-437.5,950)	54- (7845,437.5,950)	64- (10045,-437.5,950)	74- (10045,437.5,950)
45- (8095,-987.5,950)	55- (8095,987.5,950)	65- (10295,-987.5,950)	75- (10295,987.5,950)
46- (8345,-437.5,950)	56- (8345,437.5,950)	66- (10545,-437.5,950)	76- (10545,437.5,950)
47- (8095,-987.5,700)	57- (8095,987.5,700)	67- (10295,-987.5,700)	77- (10295,987.5,700)
48- (8095,-1187.5,700)	58- (8095,1187.5,700)	68- (10295,-1187.5,700)	78- (10295,1187.5,700)
49- (8095,-1187.5,0)	59- (8095,1187.5,0)	69- (10295,-1187.5,0)	79- (10295,1187.5,0)
50- (8095,-437.5,950)	60- (8095,437.5,950)	70- (10295,-437.5,950)	80- (10295,437.5,950)

Figure 2.7 Third and fourth axles hardpoints

Hardpoint locations are coming directly from vehicle's free body diagram, that will affect suspension kinematics, primarily. Suspension kinematics will play the major part for vehicle dynamics with primary and secondary suspension system coefficients.

CHAPTER THREE
FINITE ELEMENT MODELING OF THE VEHICLE

Vehicle is modeled in ANSYS according to the hardpoints of the vehicle that is specified from free body diagram of the vehicle, mentioned in previous chapter.

3.1 Creating FEA Model of the Vehicle in ANSYS

Crew cabin and Superstructure is located on the frame via secondary suspension system according to dimensions given in Figure 2.1.

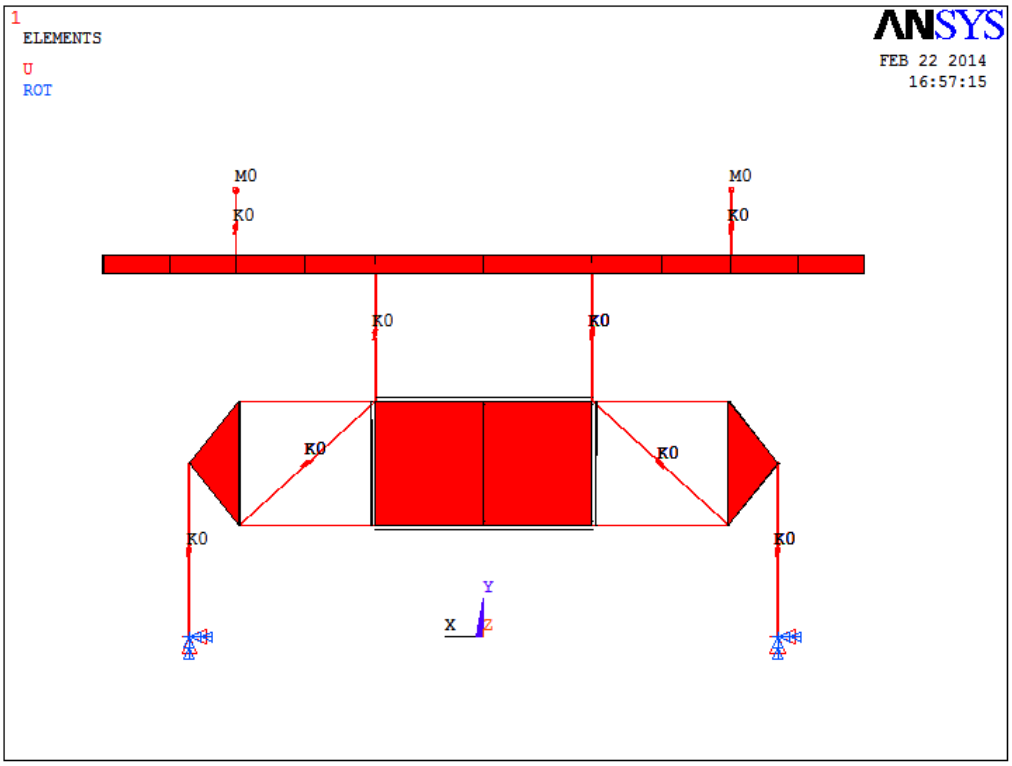

Figure 3.1 Front view of ANSYS FEA model

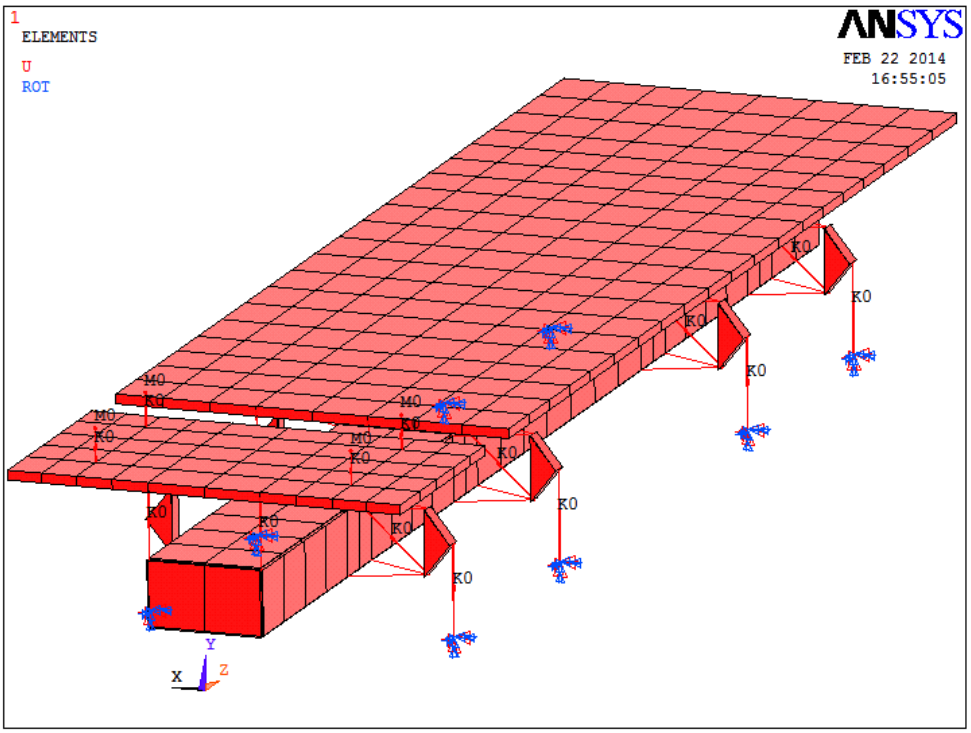

Figure 3.2 Perspective view of ANSYS FEA model

Passenger and payload are defined as mass21, spring-damper elements are defined as combin14, primary suspension lower and upper control arms are defined as mpc184,1 , vehicle frame, cabin and superstructure (cargo bed) are defined as shell63 elements. Model parameters used in the model are listed in Table 3.1 and Table 3.2 ;

Table 3.1 Model parameters

Number of Nodes	583
Number of Keypoints	149
Number of Elements	492
Number of Real Constants	11
Number of Element Types	4
Number of Materials	4
Number of Areas	149

Table 3.2 Elements used in ANSYS FEA model

Segment	***Elements used in ANSYS FEA model***
Frame	Shell63
Crew Cabin	Shell63
Superstructure(Cargo Bed)	Shell63
Payload	mass21
Driver & Passenger	mass21
Primary Suspension System Control Arms	mpc184,1
Primary & Secondary Suspension Spring-Damper Elements	combin14

CHAPTER FOUR
MODAL ANALYSIS OF THE SYSTEM AND PROVING GROUND ROAD EXCITATIONS

4.1 Modal Analysis of the System

However vehicle has quite more frequency responses when we decided that it is modeled as shell elements, crew cabin and frame natural frequencies will be considered and will be taken into account via FEA model as it is introduced in Figure1.1 Flow chart of the study in order to check the situation of the vehicle's dynamic behaviour. So considered frequencies' eigenvalues and time increments will be used as inputs for proving ground road excitations. Natural frequencies are examined in four sections as given Figure 4.1;

- Roll : Rotation of the system around Z axis in ANSYS model coordinate system
- Pitch : Rotation of the system around X axis in ANSYS model coordinate system
- Yaw : Rotation of the system around Y axis in ANSYS model coordinate system
- Bounce : Vertical movement of the system in Y axis

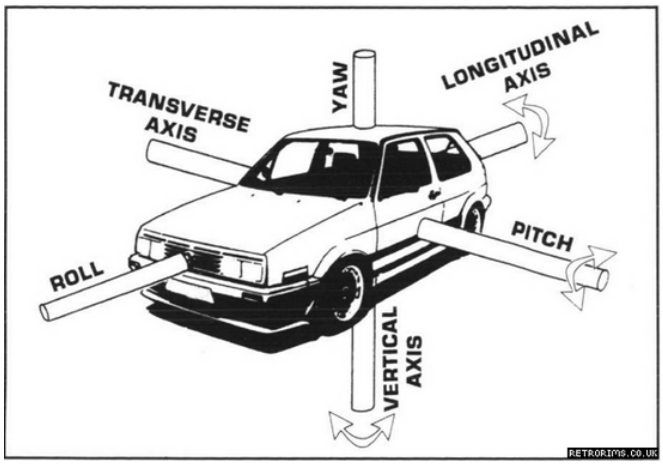

Figure 4.1 Roll, pitch, yaw axis

Because of modeling the passenger seats' attachments as spring-damper elements, couple of frequency responses may occur during different multi body motions.

Table 4.1 Natural frequencies and eigenvalues

Motion	***Description***	***Natural Frequency***	***Eigenvalues***
Roll	Relative motion of Cabin-Passenger	f=1.2319 Hz	-2.0332 ± 7.4682i
	Simultaneous motion of Cabin-Passenger	f=0.59073 Hz	-0.4670 ± 3.6819 i
Pitch	Relative motion of Cabin-Passenger	f=1.058 Hz	-1.4561 ± 6.2882i
	Simultaneous motion of Cabin-Passenger	f=1.8403 Hz	-5.5893 ±10.1046i
Bounce	Relative motion of Cabin-Passenger	f=1.3101 Hz	-2.4766 ± 7.8345i
	Simultaneous motion of Cabin-Passenger	f=0.83343 Hz	-1.1053 ± 5.1293i
Yaw	Relative motion of Cabin-Passenger	f=0.19663 Hz	0 ± 1.2355i
Passenger Bounce	Relative motion of Passengers	f=1.0864 Hz	-1.5624 ± 6.6451i
Combined Motion	Integrated motion of frame, cabin and passengers	f=3.4781 Hz	-0.5270 ± 21.8479i

According to Table 4.1 and Table 4.2, relative motion of cabin-passenger shows us the reverse movements of the cabin structure and the passengers; means, while cabin moves upwards, passengers move downwards. Simultaneous motion shows us the motion on same direction for cabin and passengers.

As it is seen in Table 4.1, all real coefficients of eigenvalues are negative. That shows us that the system is stable, and model seems reliable for the beginning.

Figure 4.2 shows the situation for the vehicle's multibody motions.

Table 4.2 Figures of natural frequencies and eigenvalues

	Relative motion Cabin-Passenger	Simultaneous motion Cabin-Passenger
Roll	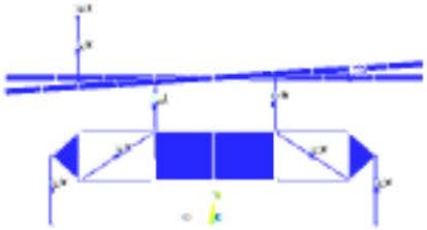	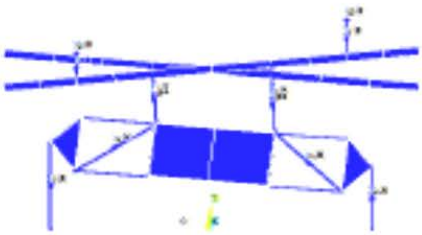
Pitch	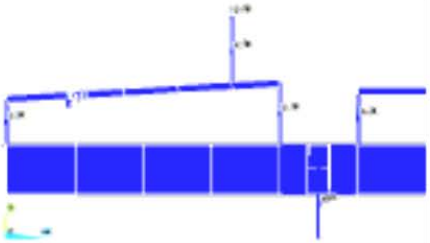	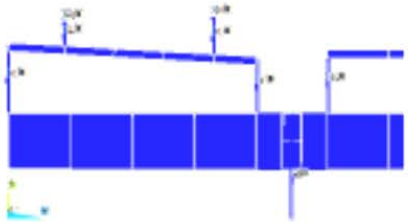
Bounce	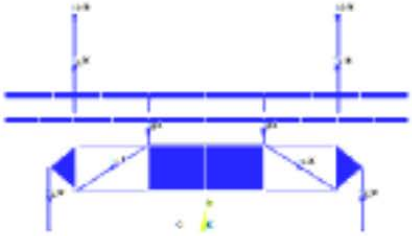	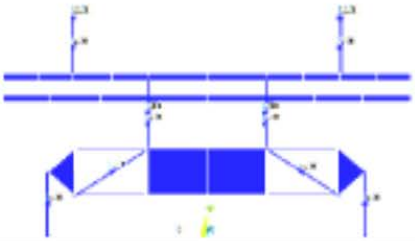
Yaw	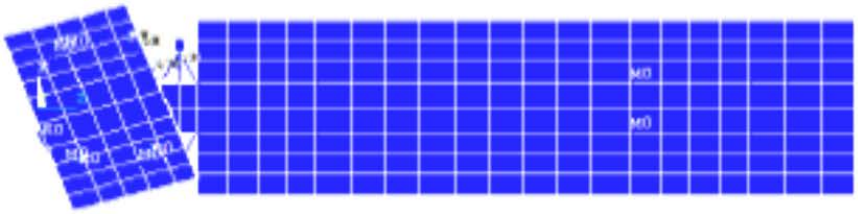	
Passenger Bounce	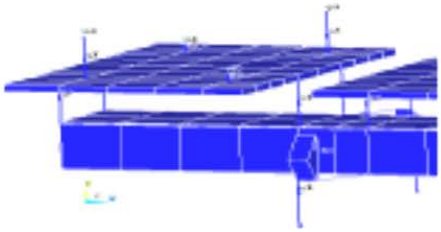	
Combined Motion	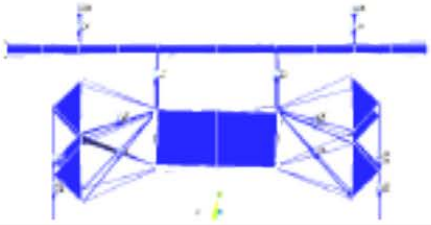	

4.2 Proving Ground Road Excitations

Real road excitations can be considered as random inputs, in this study a few conditioned road excitations is decided to be applied to the vehicle model in order to observe the vehicle's analytic responses. Thus, the responses will be observed as the vehicle is tested on the real proving ground. Three road conditions are determined, which are assumed as giving deep understanding of the vehicle's dynamic characteristics. These road conditions are listed below;

- Single Wheel Obstacle Transition
- All Wheel Obstacle Transition
- Relative Sinusoidal Obstacle Transition

4.2.1 Modeling Proving Ground Conditions

4.2.1.1 Single Wheel Obstacle Transition

Vehicle's left wheels will go over a 10 cm height and 10.5m length obstacle and then fall again to the starting groundline with a 36km/h velocity. Excitation time for each wheels will increase proportional to the wheelbase dimension, while going backside of the vehicle.

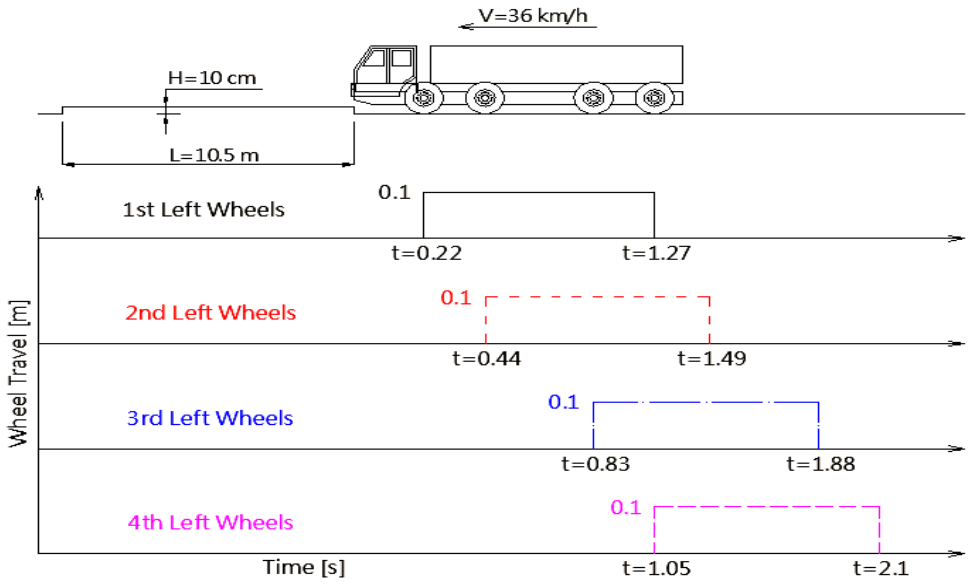

Figure 4.2 Side view of the obstacle & wheel travel-time graph of each left wheels

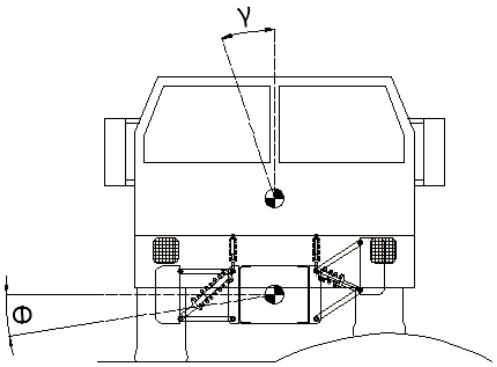

Figure 4.3 Front view of the obstacle

In Figure 4.2, vehicle is shown 2.2m away from the obstacle, and approaching with 36 km/h velocity. If we accept t=0 at this instant, first left wheel will be exposed by first base excitation at t=0.22s ,and then other wheels will be exposed at t=0.44, t=0.88, t=1.05 respectively. Durations is 1.05 seconds for all wheels to pass over the obstacle.

4.2.1.2 All Wheel Obstacle Transition

All vehicle tires will go over a 10 cm height and 10.5m length obstacle and then fall again to the starting groundline with a 36km/h velocity. Two wheels on the same axle will go over the obstacle simultaneously.

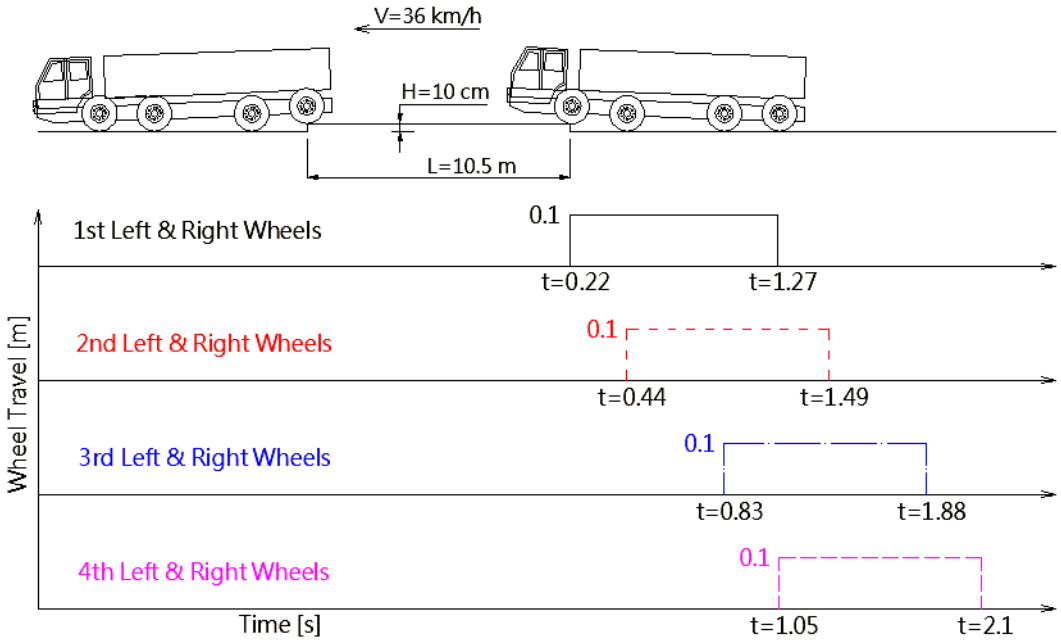

Figure 4.4 Side view of the obstacle & wheel travel-time graph of each wheels

The situation is the same as Figure 4.2. First base excitation is exposed at t=0.22 seconds for both wheels of an axle, wheels at second axle are excited at t=0.44, wheels at third axle are excited at t=0.83, and wheels at fourth axle are excited at t=1.05 seconds as shown in Figure 4.4.

Length of the obstacle and the vehicle speed is the same as previous proving ground scenario, so the duration of the vehicle passing over the obstacle is also the same as previous one.

4.2.1.3 Relative Sinusoidal Obstacle Transition

Vehicle will go over a sinusoidal obstacle and then fall again to the starting groundline with a 36km/h velocity. Two wheels will go over the obstacle relatively, means while one wheel is climbing upwards, other wheel is moving downwards during passing the obstacle, on each axles.

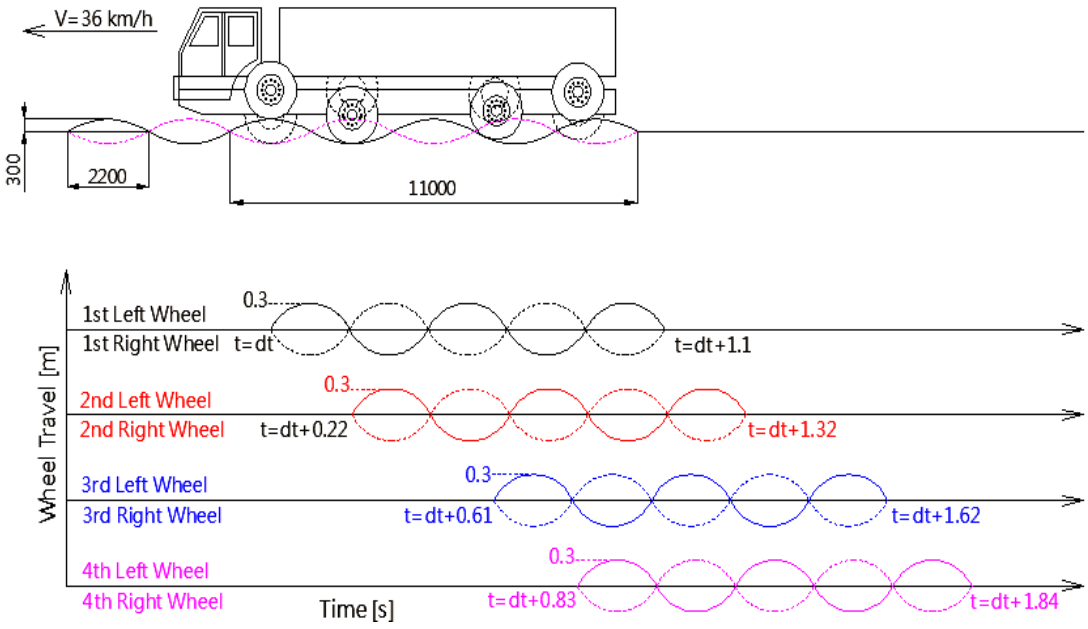

Figure 4.5 Side view of the obstacle & wheel travel graph of each left and right wheels

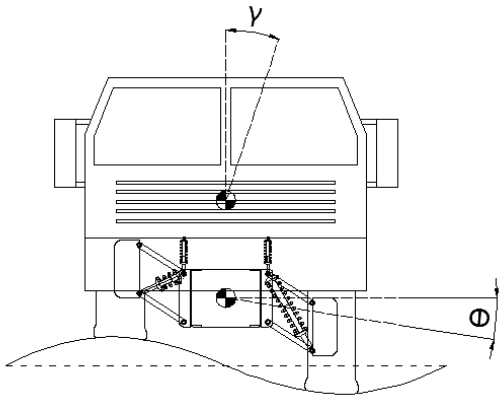

Figure 4.6 Front view of the obstacle

First base excitation is assumed to be exposed at t=dt, where dt will be calculated in next sections according to vehicle's modal response. Vehicle's velocity is 36km/h, so other wheels' excitations will be 0.22, 0.61, 0.83 seconds later than the first excitation occurred.

Excitation duration seems dt+1.84 seconds, according to the length of the obstacle. Formulation of the road profile is given below. Matlab codes are given in Appendix.

$y_1 = 0.3 \sin(1.428t)$ for left tires

$y_2 = 0.3 \cos(1.428t + \pi/2)$ for right tires

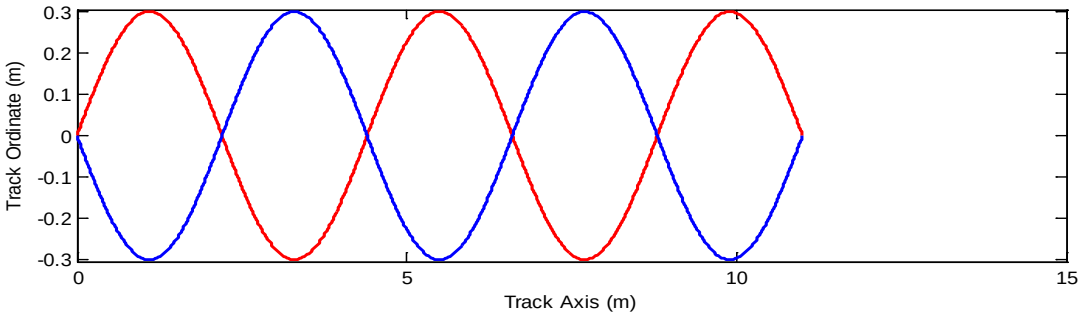

Figure 4.7 Relative sinusoidal road profiles

4.2.2 Calculation of Dynamic Analysis Parameters From Modal Analysis Results

Vehicle responses will be defined from ANSYS model for all proving ground road excitations. For relevant motion, eigenvalue of the related modes will be taken

from Table 4.1 and time increments will be calculated to be used as inputs during FEA simulations.

Once the eigenvalue for each motion is defined, system period, frequency, time increment and settling time are calculated according to the formulas given below.

$$p0 = a + bi \tag{4.1}$$

$$T = 2\pi/\sqrt{a^2 + b^2} \ : Period\ of\ the\ system \tag{4.2}$$

$$f = 1/T : Frequency\ of\ the\ system \tag{4.3}$$

$$dt = T/20 : Time\ increment \tag{4.4}$$

$$t_{inf} = T/\left(a/\sqrt{a^2 + b^2}\right) : Infinite\ time \tag{4.5}$$

Eigenvalues will be defined for all proving ground excitations, respectively. All parameters will be calculated accordingly.

4.2.2.1 Dynamic Analysis Parameters For Single Wheel Obstacle Transition

Vehicle response is defined from ANSYS model as shown in Figure 4.8, and Figure 4.9. Eigenvalues of the system and dynamic analysis parameters for this mod is;

p0 = -0.4670 ± 3.6819 i ; (4.6)

T = 1.6929 s

f = 0.59073 Hz

dt = 0.0846 s

t_{inf} = 13.4544 s

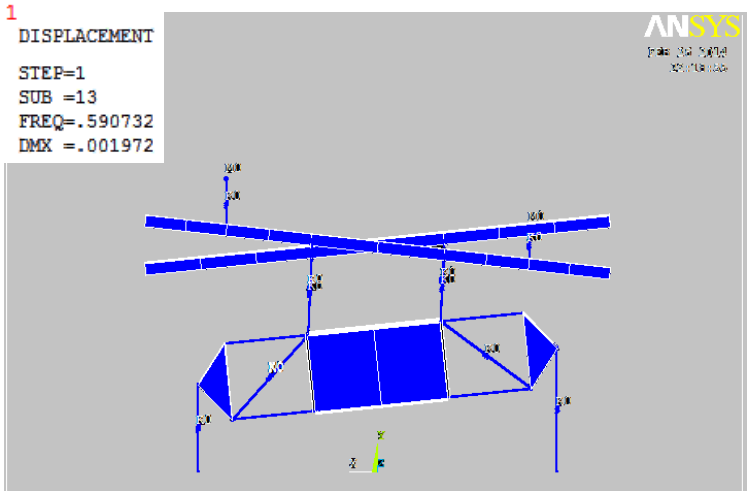

Figure 4.8 Front view of vehicle response for single wheel obstacle transition

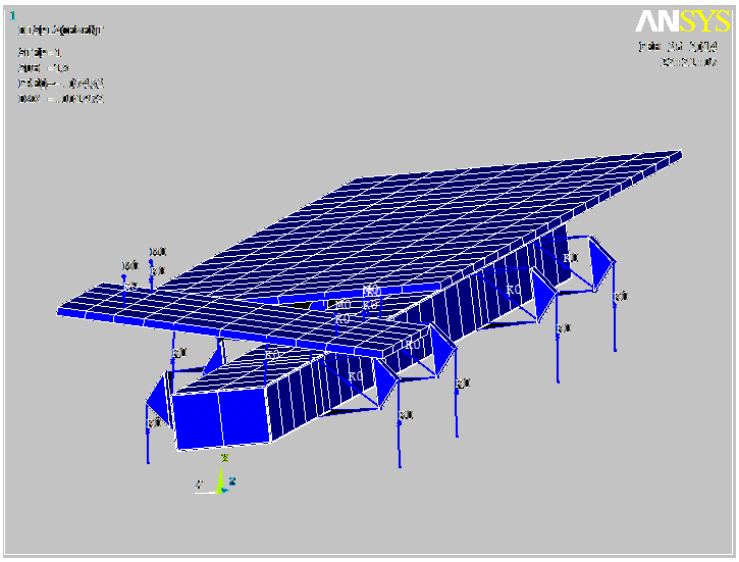

Figure 4.9 Perspective view of vehicle response for single wheel obstacle transition

4.2.2.2 Dynamic Analysis Parameters For All Wheel Obstacle Transition

Vehicle response is defined from ANSYS model as shown in Figure 4.10, and Figure 4.11. Eigenvalues of the system and dynamic analysis parameters for this mod is;

$$p0 = -1.1053 \pm 5.1293i \tag{4.7}$$

$T = 1.1975$ s

$f = 0.83343$ Hz

dt = 0.0599 s

t_{inf} = 5.6846 s

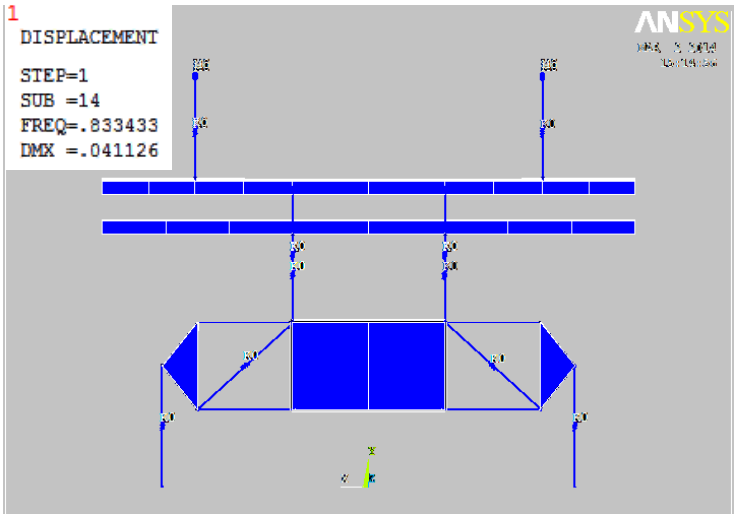

Figure 4.10 Front view of vehicle response for all wheel obstacle transition

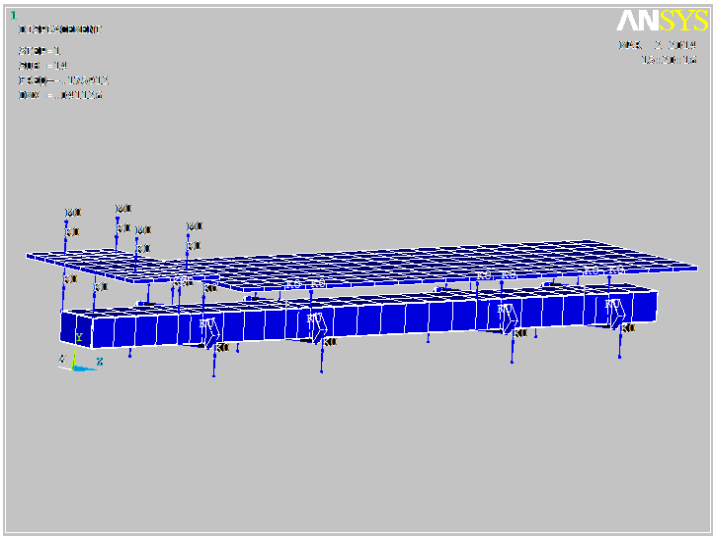

Figure 4.11 Perspective view of vehicle response for all wheel obstacle transition

4.2.2.3 Dynamic Analysis Parameters For Relative Sinusoidal Obstacle Transition

Vehicle response is defined from ANSYS model as shown in Figure 4.12, and Figure 4.13. Eigenvalues and dynamic analysis parameters of the system for this mod is;

$p0 = -0.5270 \pm 21.8479i$ (4.8)

$T = 0.2875$ s

$f = 3.4781$ Hz

$dt = 0.0144$ s

$t_{inf} = 11.9226$ s

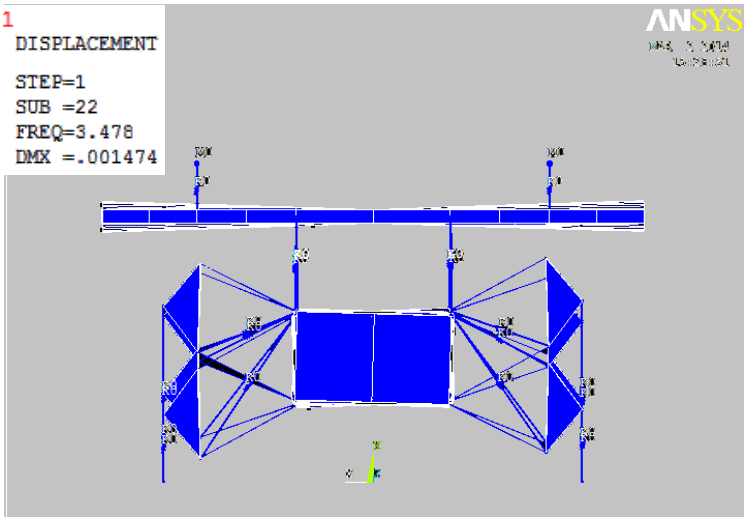

Figure 4.12 Front view of vehicle response for relative sinusoidal obstacle transition

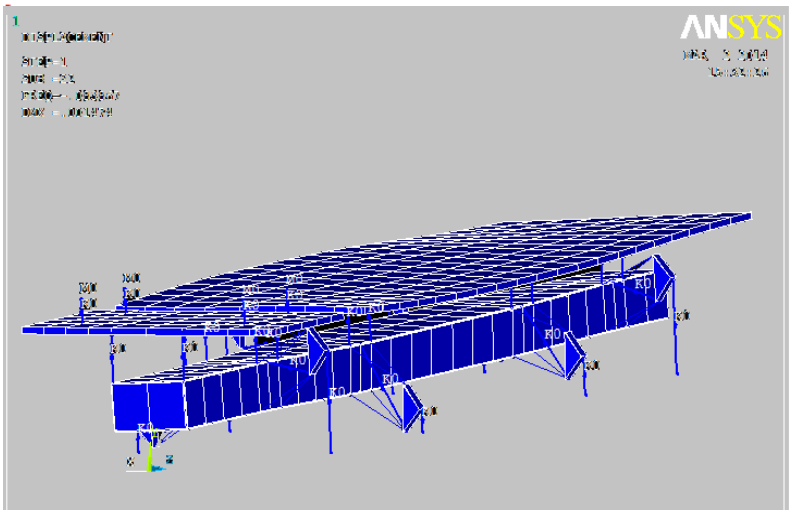

Figure 4.13 Perspective view of vehicle response for relative sinusoidal obstacle transition

For all three proving ground road conditions, roll, bounce and pitch reactions of the vehicle will be observed, respectively in next chapter.

CHAPTER FIVE
DYNAMIC RESPONSES OF THE VEHICLE ACCORDING TO PROVING GROUND ROAD EXCITATIONS

Simulations are performed by using the specified modal responses defined in Chapter 4 as inputs. In this chapter, it will be interested with the displacement, velocity and acceleration versus time values of the given nodes. Roll, bounce and pitch responses of crew cabin, passengers and vehicle frame will be calculated respectively for the proving ground road excitations. Dynamic responses of the vehicle will be examined via the nodes given below.

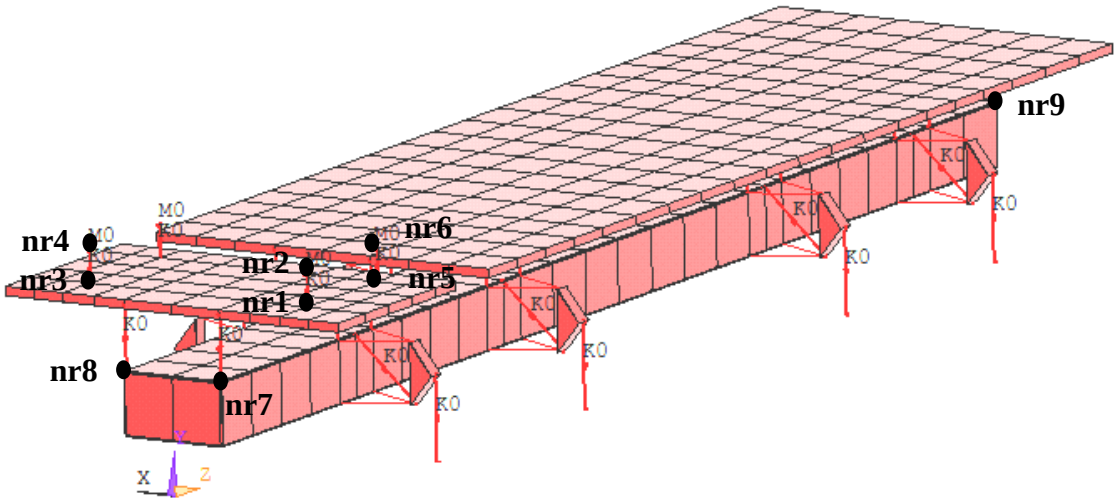

Figure 5.1 Dynamic Response nodes

Table 5.1 . Dynamic Response nodes

nr1	Driver Cabin Node	nr2	Driver Seat Node
nr3	Commander Cabin Node	nr4	Commander Seat Node
nr5	LHS Passenger Cabin Node	nr6	LHS Passenger Seat Node
nr7	Front LHS Frame Node	nr8	Front RHS Frame Node
nr9	Rear End LHS Frame Node		

Vehicle nodal response will be examined via the given nodes in Figure 5.1 and Table 5.1 for each of the cases defined as proving ground road excitations. Calculation method is as described below;

- FE model of the vehicle is prepared as described in Chapter 3.
- Proving Ground (PG) road excitations are defined for all three cases in Chapter 4.
- Time increments are calculated via the mode shapes of PG road excitations in Chapter 4.
- Defined PG excitations are applied to FEA simulations, in order to present the nodal dynamic responses to be mentioned in this Chapter, for each PG road case by using calculated time increments.
- Nodal responses will be presented and examined as the result of FE simulations.

Keypoint of this study can be explained as exciting the FE model on correct mode shape. We can only comment the results truly, by performing the simulations for each PG case, by applying the input of the mode shape that the system is excited on. Thus, applying the correct time increment has the major effect on this study.

Mode shapes are defined for each PG conditions below, and dynamic responses for each PG conditions will be presented in following sections.

- Single Wheel Obstacle Transition : Roll mode is performed. Road excitation is applied as given in Appendix 1.3.1. Eigenvalues and modal parameters are given in Section 4.2.2.1. Finally FEA analysis is performed in ANSYS.
- All Wheel Obstacle Transition : Bounce mode is performed. Road excitation is applied as given in Appendix 1.4.1. Eigenvalues and modal parameters are given in Section 4.2.2.2. Finally FEA analysis is performed in ANSYS.
- Sinusoidal Obstacle Transition : Pitch and yaw modes are performed. Sinusoidal road profiles for left and right wheels are generated in Matlab as given in Appendix. These profiles are adapted according to vehicle velocity again in Matlab. A text file generated from Matlab code is used as primary input, and the values in text file is transformed to the road excitations via compilaton in Visual Basic as given in

Appendices 1.6.1, 1.6.2, 1.6.3, 1.6.4, 1.6.5, 1.6.6, 1.6.7, 1.6.8. Eigenvalues and modal parameters are given in Section 4.2.2.3. Finally FE analysis is performed in ANSYS.

5.1 Dynamic Responses of the Vehicle For Single Wheel Obstacle Transition

Crew cabin, passenger and vehicle frame responses will be checked for both left and right hand side of the vehicle. Hereby, roll motions will be found by using the left and right hand side responses. Data are collected from ANSYS FE model from the nodes, shown in Figure 5.1.

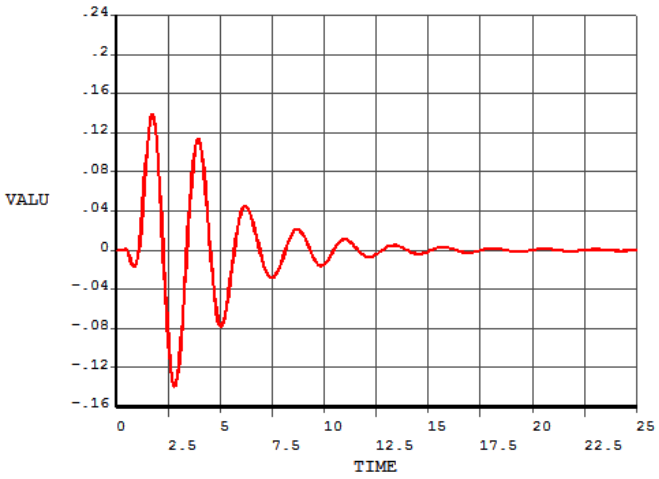

Figure 5.2 nr1 displacement-time graph

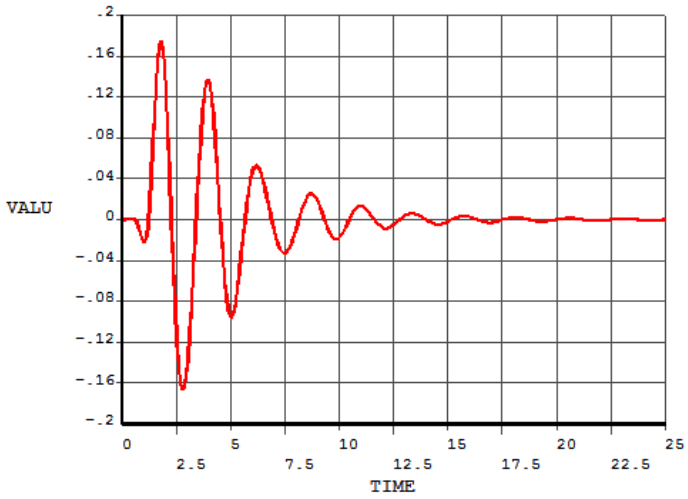

Figure 5.3 nr2 displacement-time graph

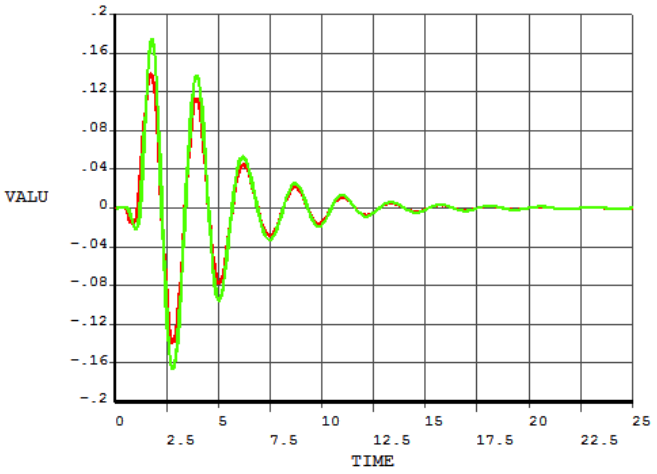

Figure 5.4 nr1/nr2 displacement-time comparison

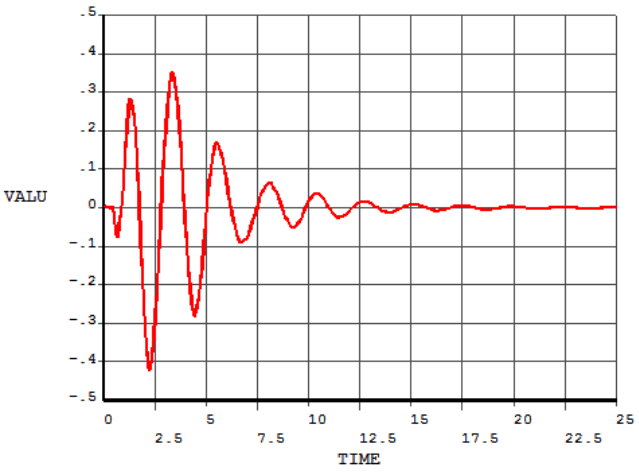

Figure 5.5 nr1 velocity-time graph

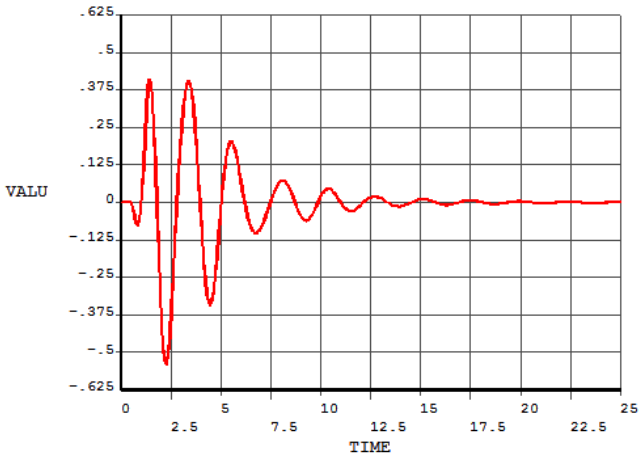

Figure 5.6 nr2 velocity-time graph

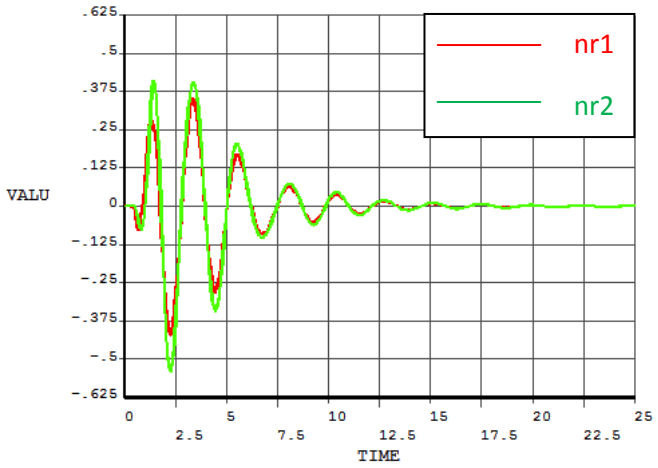

Figure 5.7 nr1/nr2 velocity-time comparison

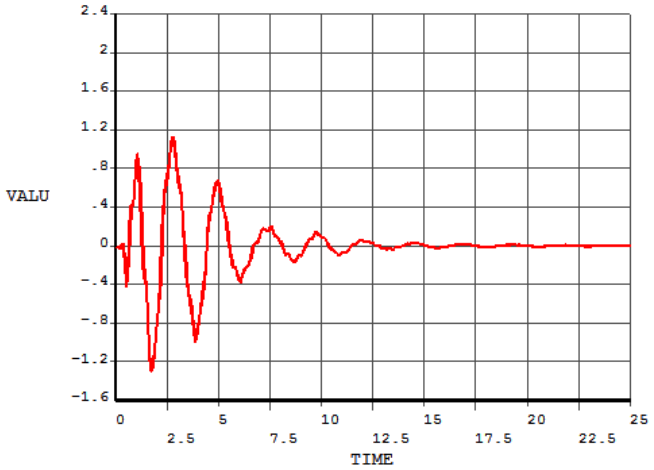

Figure 5.8 nr1 acceleration-time graph

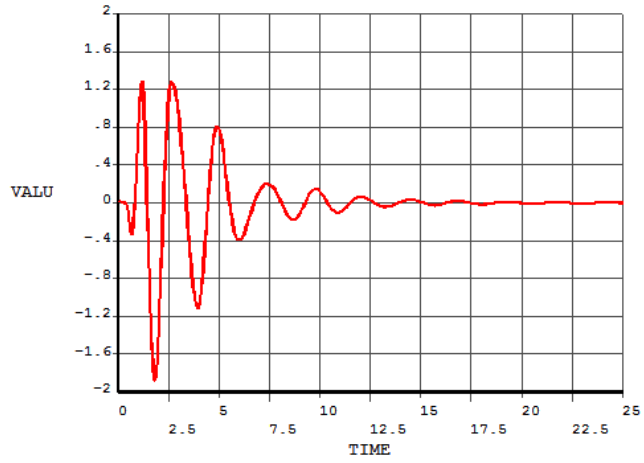

Figure 5.9 nr2 acceleration-time graph

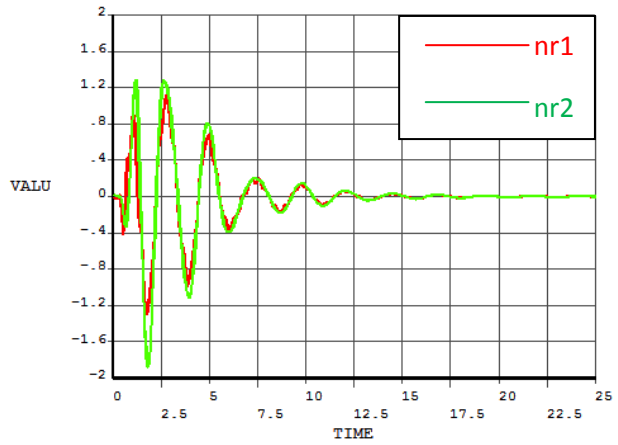

Figure 5.10 nr1/ nr2 acceleration-time comparison

Above figures between Figure 5.2 and Figure 5.10, gives us bounce motion details of the crew cabin and passenger seat nodes at the driver side. However motion amplitudes are different, both nodes move synchronously. Parameters of Spring-Damper element between the cabin and driver seat allows the driver move more freely than the crew cabin, on the other hand vehicle's ride will be under driver's control because driver moves on the same phase angle with the crew cabin. In order to check the roll motion of the cabin, we will look at the bounce of commander side (nr3). Difference between the nodes nr1 and nr3 will give us a necessary parameter for calculating the crew cabin roll response.

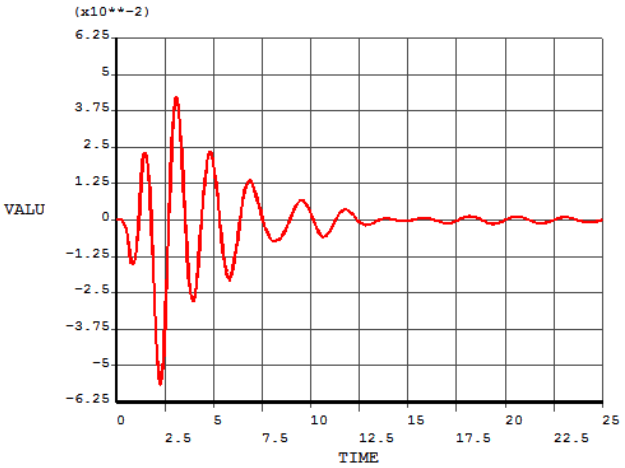

Figure 5.11 nr3 displacement-time graph

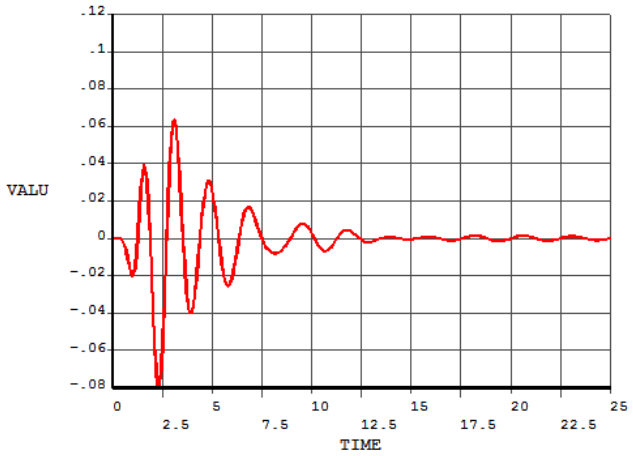

Figure 5.12 nr4 displacement-time graph

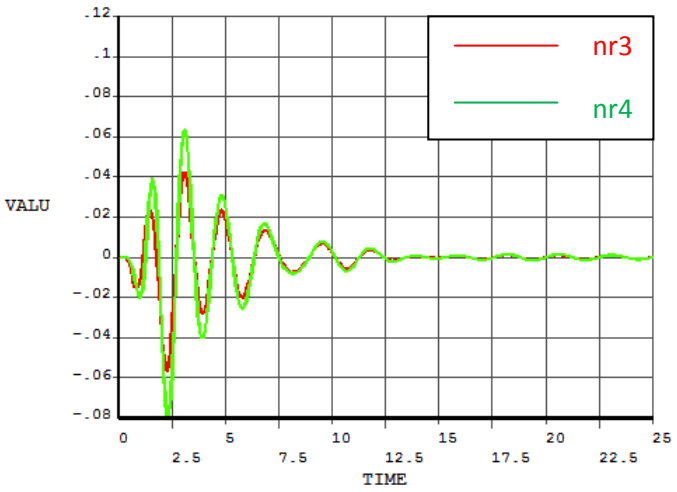

Figure 5.13 nr3/nr4 displacement-time comparison

Figure 5.13 shows us, passenger and crew cabin response characteristics on the commander side (RHS of vehicle) are the same as the driver side (LHS of vehicle). They also move on the same phase angle. We will compare the graphic results of Figure 5.2 and Figure 5.11 for the roll characteristic of the crew cabin.

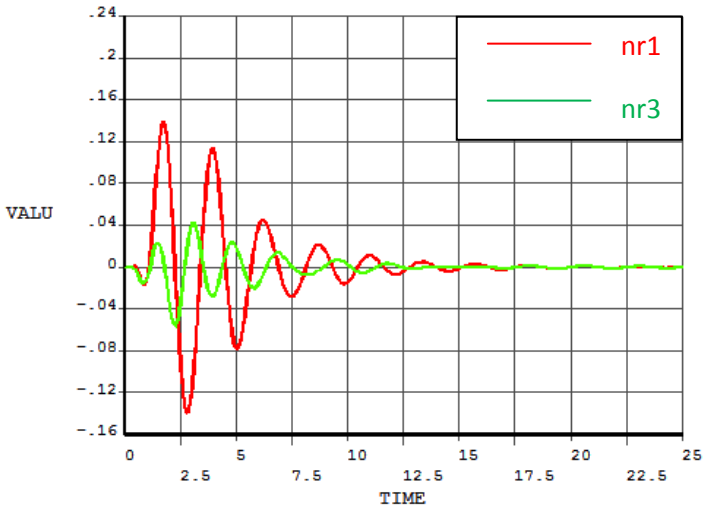

Figure 5.14 nr1/nr3 displacement-time comparison

Figure 5.14, which is a mix of Figure 5.2 and Figure 5.11 shows us that the driver side (LHS) and commander side (RHS) bounce with different amplitudes and phase angle. So, this means cabin is doing a roll movement during passing the obstacle.

Crew Cabin Roll angle "γ" can be calculated via using the parameters given in Figure 5.15 .

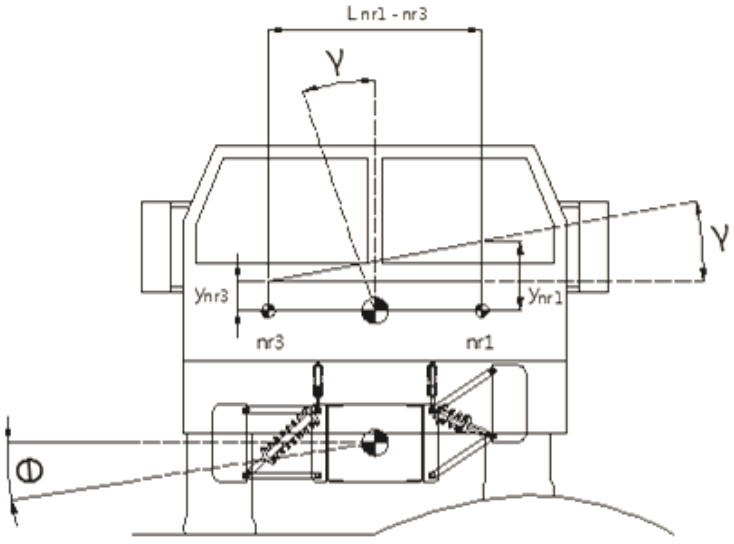

Figure 5.15 Crew cabin roll parameters

$$\gamma = tan^{-1}\left(\frac{y_{nr1}-y_{nr3}}{L_{nr1-nr3}}\right) \quad (5.1)$$

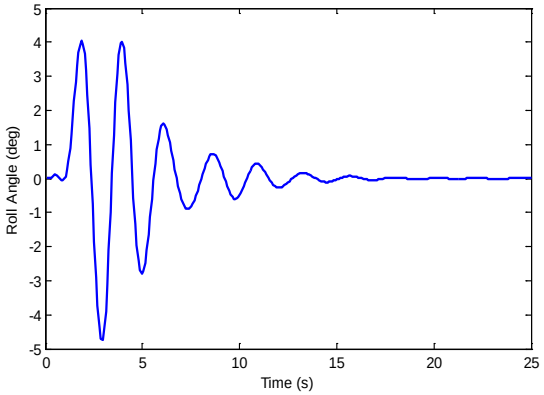

Figure 5.16 crew cabin roll angle - time graph

Displacement-time graph belongs to nodes nr5 and nr6 will be figured and compared with nr1 in order to check the pitch motion of crew cabin.

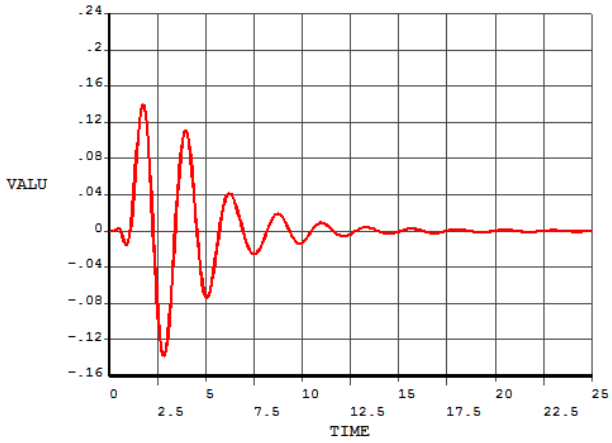

Figure 5.17 nr5 displacement-time graph

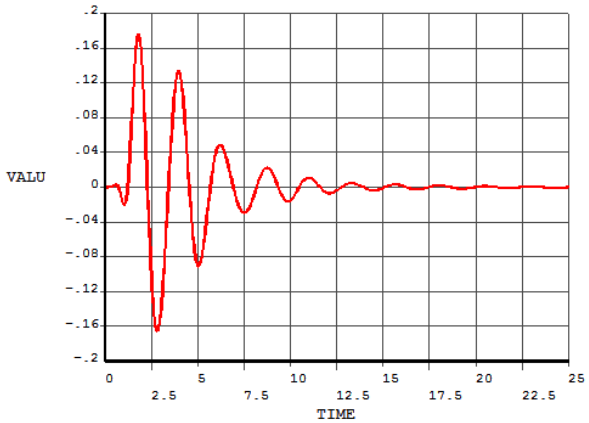

Figure 5.18 nr6 displacement-time graph

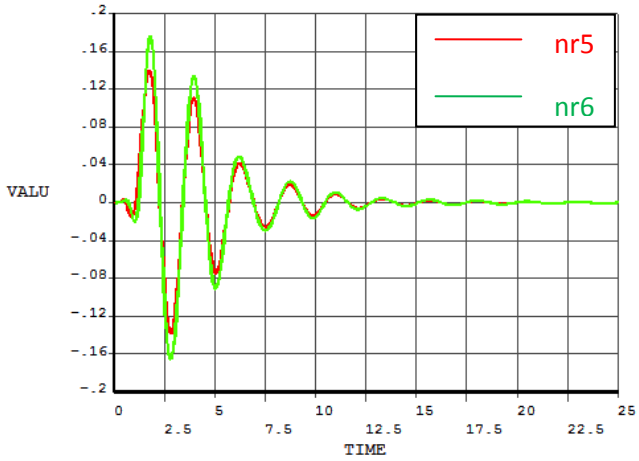

Figure 5.19 nr5/nr6 displacement-time comparison

Bounce situation is the same for nodes nr5 and nr6. They have different displacement amplitudes but they move on the same phase angle. Nodes nr1 and nr5 will be compared for the crew cabin pitch motion.

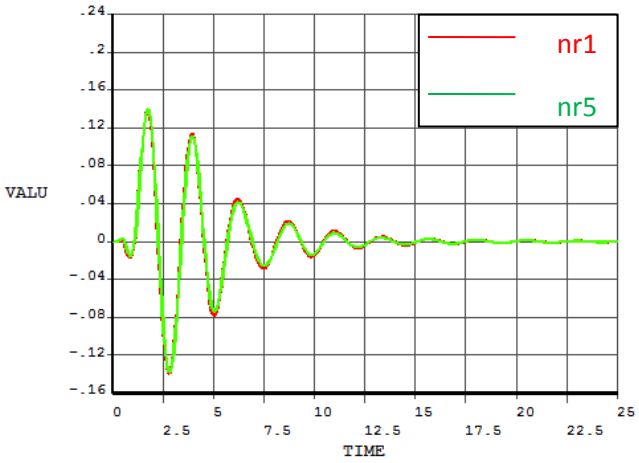

Figure 5.20 nr1/nr5 displacement-time comparison

Figure 5.20 shows us bounce amplitude difference between nodes nr1 and nr5 is nearly negligible, and phase angles of two nodes are almost the same. We will check the level of pitch motion by using below parameters.

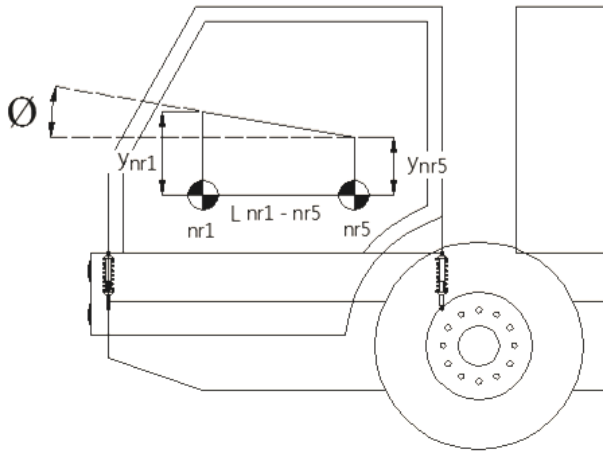

Figure 5.21 Crew cabin pitch parameters

$$\emptyset = tan^{-1}\left(\frac{y_{nr1}-y_{nr5}}{L_{nr1-nr5}}\right) \tag{5.2}$$

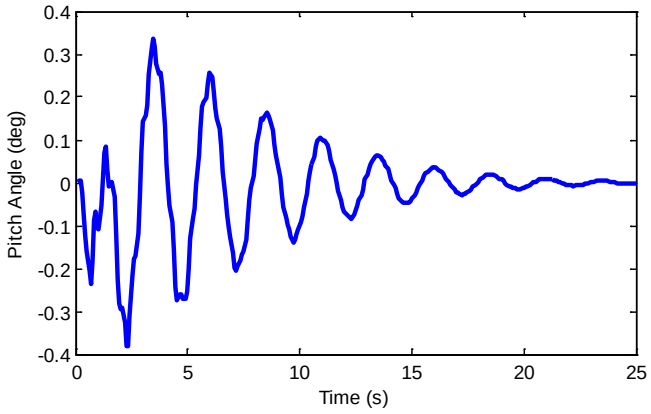

Figure 5.22 Cabin Pitch angle - time graph

As shown in Figure 5.22, max pitch angle is calculated as "0.3355°" which can be neglected for human perception.

Finally, we will examine the frame bounce and roll behaviors. A comparison between frame and cabin will also be performed to double check if the cabin suspension elements damp the excitations or allow the cabin move more free than the vehicle frame.

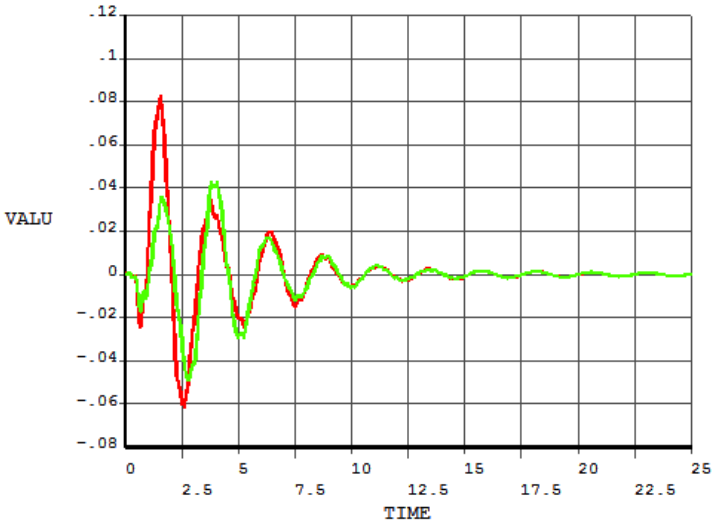

Figure 5.23 nr7/nr8 displacement-time comparison

Figure 5.23 shows that, LHS and RHS of the frame move with the same phase angle, but bounce amplitudes are different. Difference will give us the roll level of the frame.

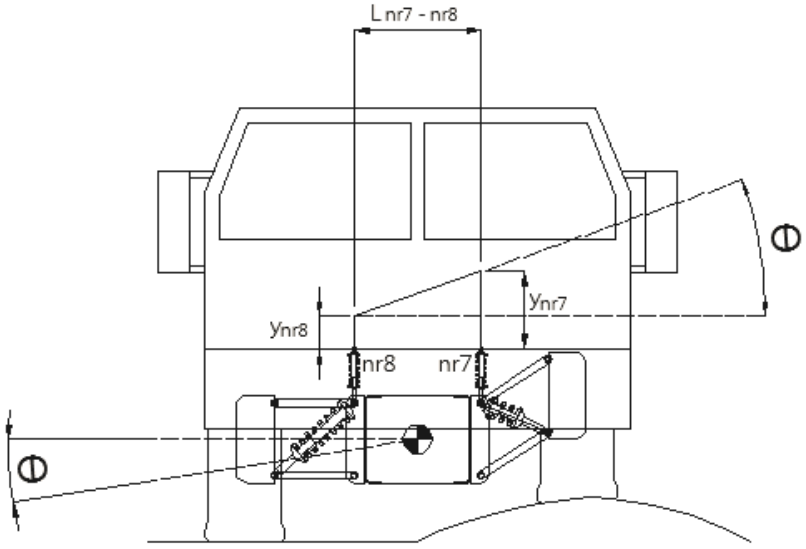

Figure 5.24 Frame roll parameters

$$\theta = tan^{-1}\left(\frac{y_{nr7}-y_{nr8}}{L_{nr7-nr8}}\right) \quad (5.3)$$

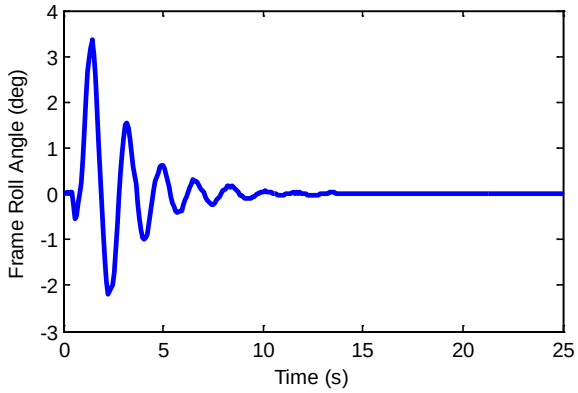

Figure 5.25 Frame roll angle - time graph

Bounce comparison will also be performed between nr1 and n7, nr3 and nr8 in Figures 5.26 and 5.27 .

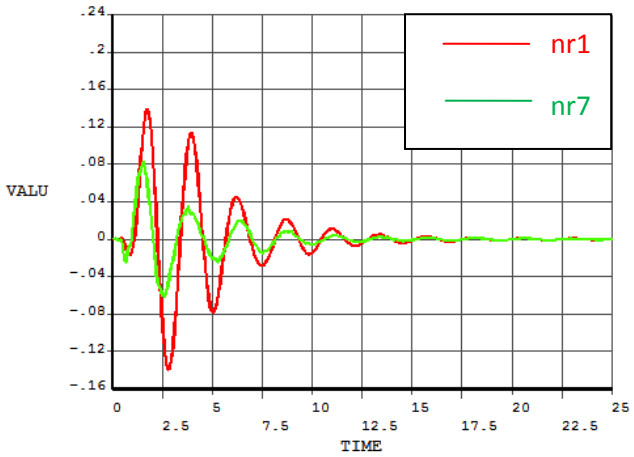

Figure 5.26 nr1/nr7 displacement-time comparison

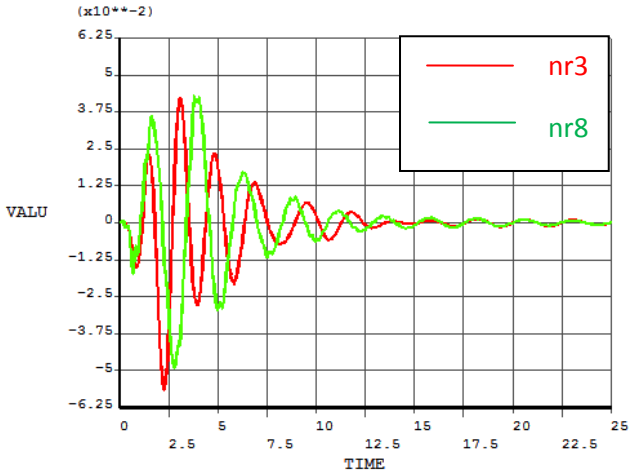

Figure 5.27 nr3/nr8 displacement-time comparison

Minimum and maximum nodal displacement, velocity and acceleration values can be checked in below tables.

Table 5.2 Nodal displacements

Nodal Displacements		
Number of Nodes	Minimum/Maximum Values (m)	
nr1	Min	-0.139184
	Max	0.138655
nr2	Min	-0.166347
	Max	0.174299
nr3	Min	-0.0564903
	Max	0.0421454
nr4	Min	-0.0782344
	Max	0.0634774
nr5	Min	-0.137576
	Max	0.139256
nr6	Min	-0.165076
	Max	0.175878
nr7	Min	-0.0611727
	Max	0.0826596
nr8	Min	-0.0490944
	Max	0.0429593

Table 5.3 Nodal Velocities

Nodal Velocities		
Number of Nodes	Minimum/Maximum Values (m/s)	
nr1	Min	-0.421162
	Max	0.350835
nr2	Min	-0.53772
	Max	0.409673

Table 5.4 Nodal Acceleration

Nodal Accelerations		
Number of Nodes	Minimum/Maximum Values (m/s^2)	
nr1	Min	-1.295
	Max	1.12181
nr2	Min	-1.87854
	Max	1.28144

Table 5.5 Dynamic Characteristics of the Vehicle

Crew Cabin Maximum Roll Angle	-4.725°
Frame Maximum Roll Angle	3.361°
Crew Cabin Maximum Pitch Angle	0.3355°

5.2 Dynamic Responses of the Vehicle For All Wheel Obstacle Transition

In this section vehicle bounce and pitch responses will be observed via ANSYS model results. So the reactions on nodes given in below figure will be examined. Pitch motion of the crew cabin and vehicle frame will also be presented.

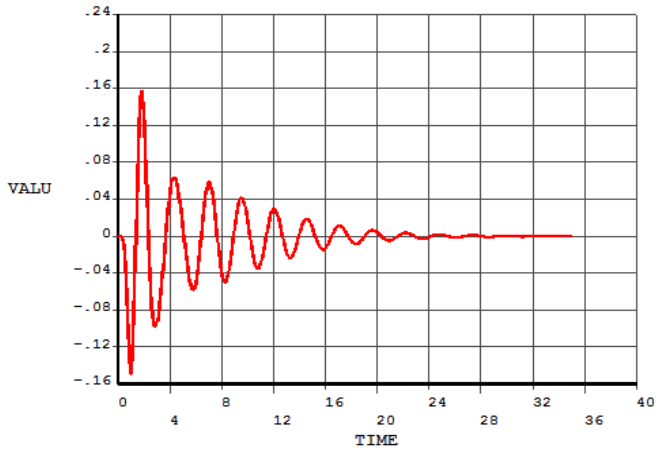

Figure 5.28 nr1 displacement-time graph

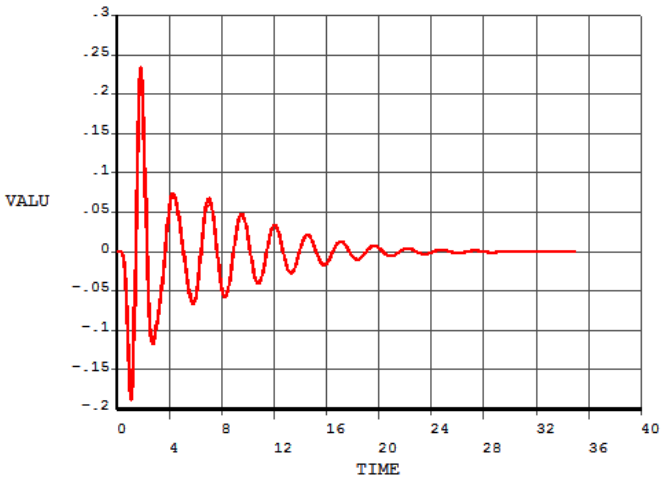

Figure 5.29 nr2 displacement-time graph

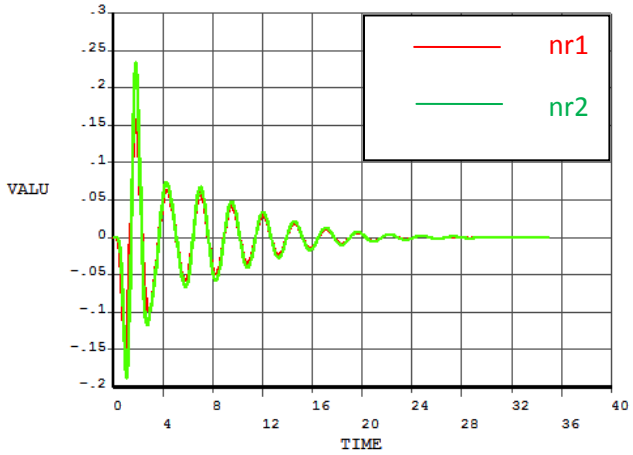

Figure 5.30 nr1/nr2 displacement-time comparison

Figure 5.29 and Figure 5.30 shows us nearly the same situation happens for the nr1 and nr2 vertical bounce motions likewise the reaction results of side step input.

Driver node has higher amplitude value than the cabin node, but they move on the same phase angle. Nodal velocity and accelerations will be checked.

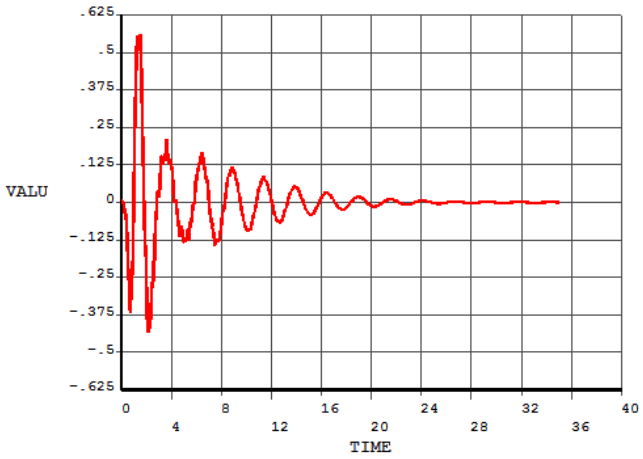

Figure 5.31 nr1velocity-time graph

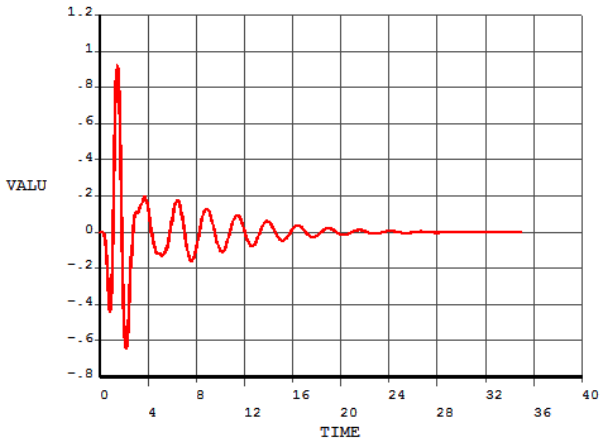

Figure 5.32 nr2 velocity-time graph

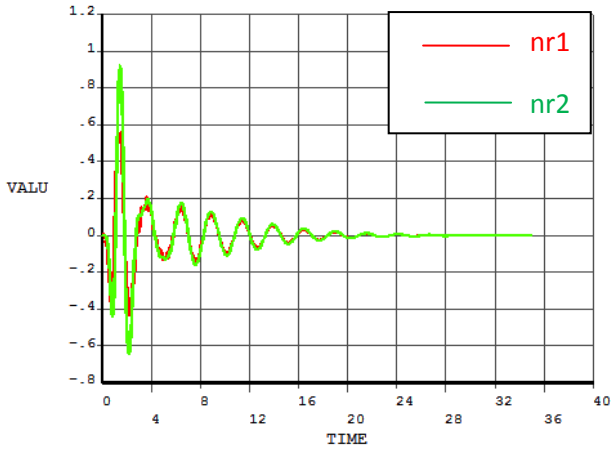

Figure 5.33 nr1/nr2 velocity-time comparison

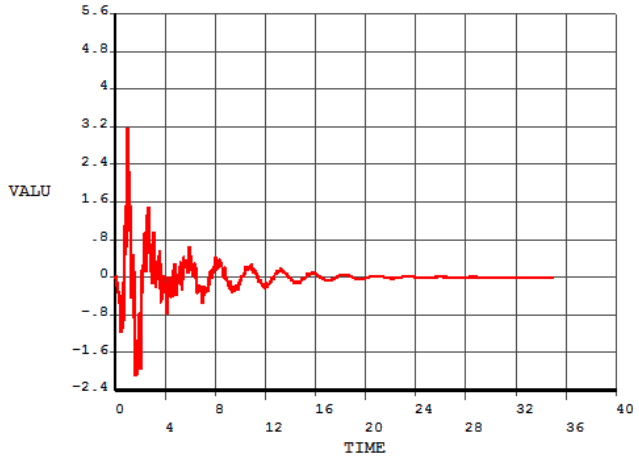

Figure 5.34 nr1 acceleration-time graph

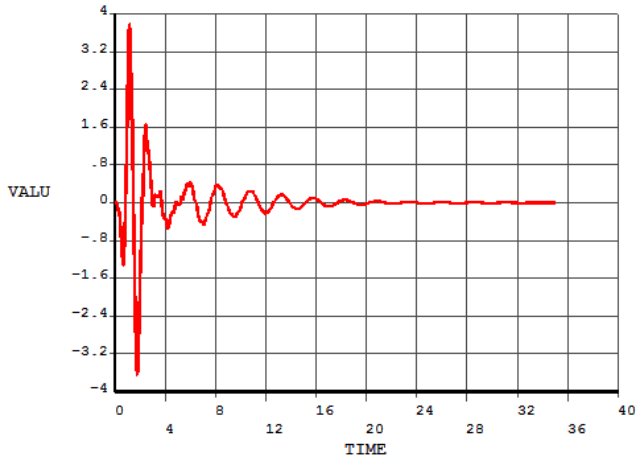

Figure 5.35 nr2 acceleration-time graph

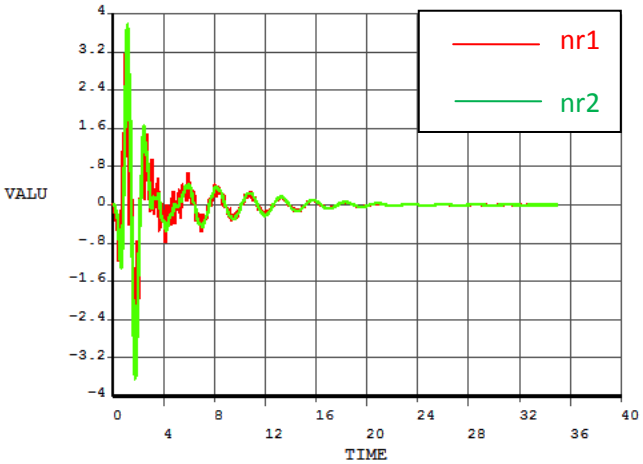

Figure 5.36 nr1/nr2 acceleration-time comparison

As it is seen from above graphics, amplitude-phase angle situation of velocity and acceleration is similar with the situation of displacement. However, some noise vibrations occur on cabin node "nr1", driver node "nr2" seems more stable, so this may be considered as a good point for the handling will be under driver's control.

Now, for the pitch motion control of the crew cabin, nr5 and nr6 nodal reactions will be checked. And the amplitude comparison between nr1 and nr5 will give an idea of the cabin pitch motion via using the calculation method described in Figure 5.21.

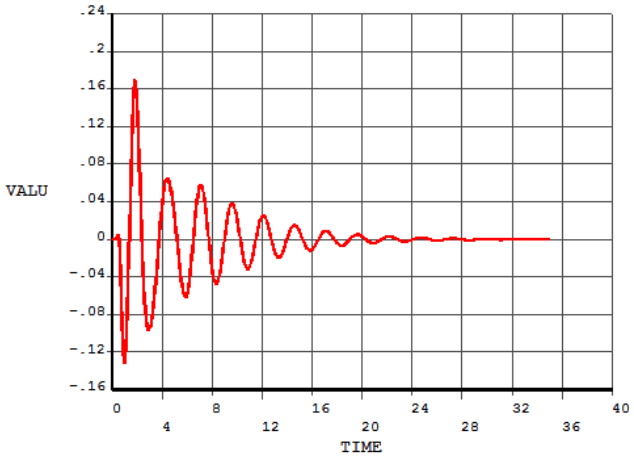

Figure 5.37 nr5 displacement-time graph

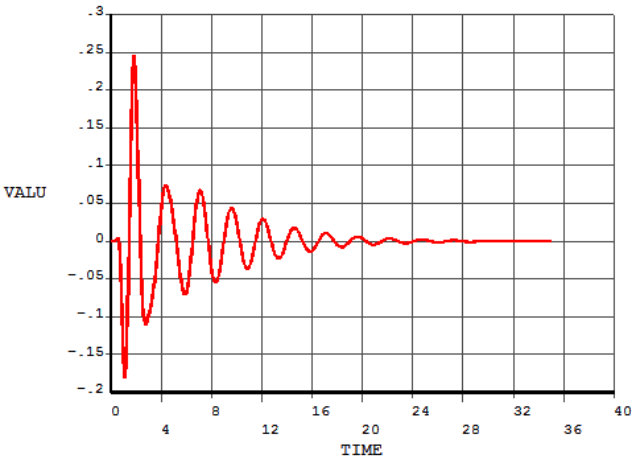

Figure 5.38 nr6 displacement-time graph

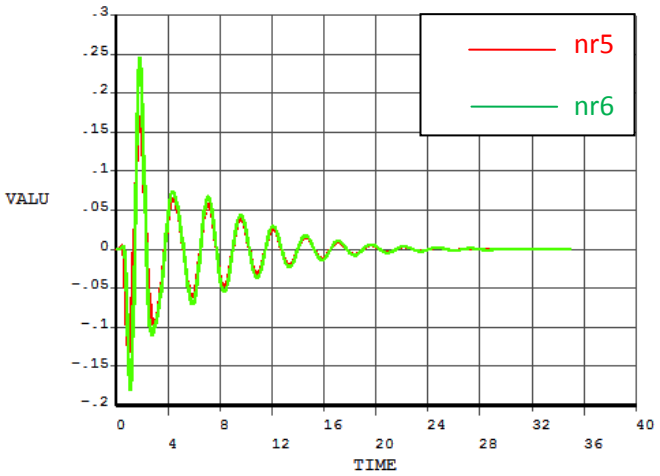

Figure 5.39 nr5/nr6 displacement-time comparison

Figure5.39 shows that the nr5 and nr6 are also moving with the same phase angle.

Nodal reactions of nr1 and nr5 will give the pitch motion of the cabin. So a comparison between the displacements of two nodes versus time will be performed in Figure 5.40 .

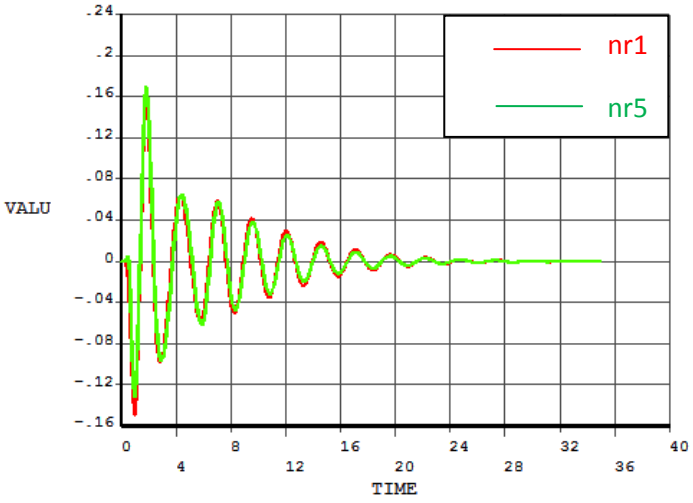

Figure 5.40 nr1/nr5 displacement-time comparison

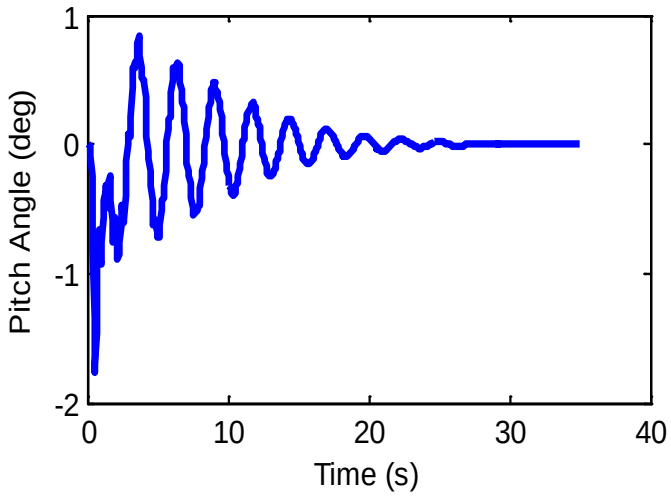

Figure 5.41 Cabin pitch angle-time graph

Figure 5.41 shows the pitch angle change of the vehicle's cabin versus time. Maximum pitch angle is -1.75° as it is seen on the graphic. This angle value corresponds a 17 mm difference on y axis.

The situation will be checked for frame nodes nr7 and nr9. Their vertical bounce and pitch characteristics will be checked via given nodal reaction results.

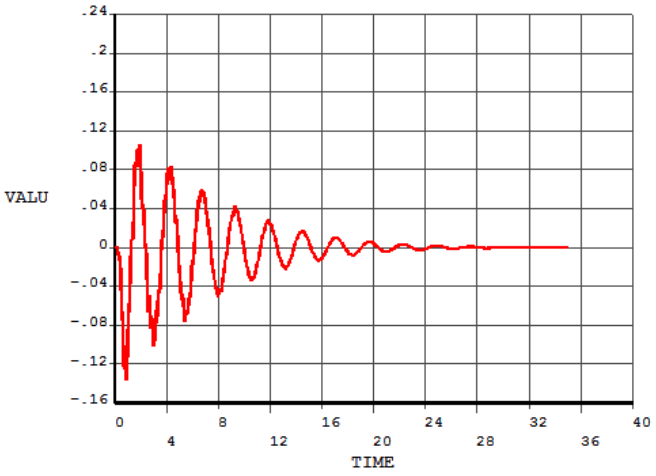

Figure 5.42 nr7 displacement-time graph

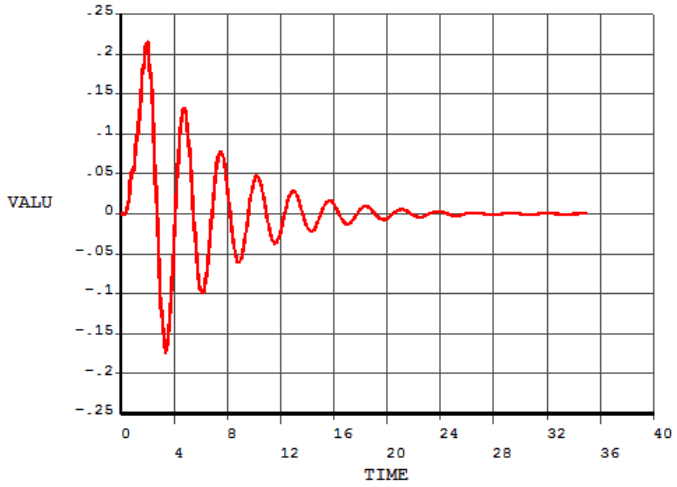

Figure 5.43 nr9 displacement-time graph

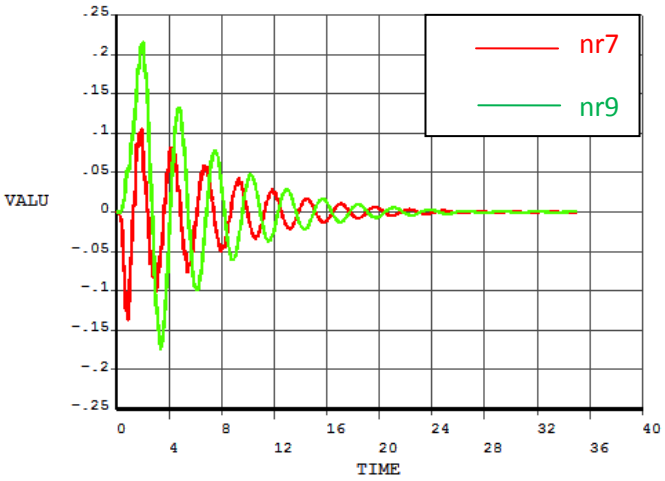

Figure 5.44 nr7/nr9 displacement-time comparison

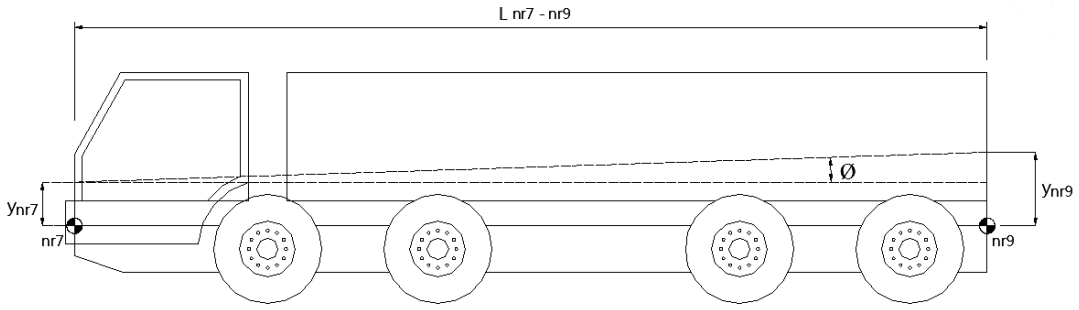

Figure 5.45 Frame pitch parameters

$$\emptyset = tan^{-1}\left(\frac{y_{nr7}-y_{nr9}}{L_{nr7-nr9}}\right) \quad (5.4)$$

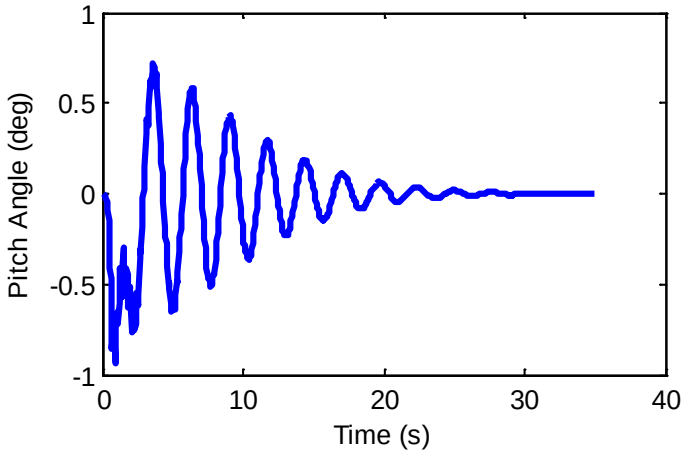

Figure 5.46 Frame pitch angle-time graph

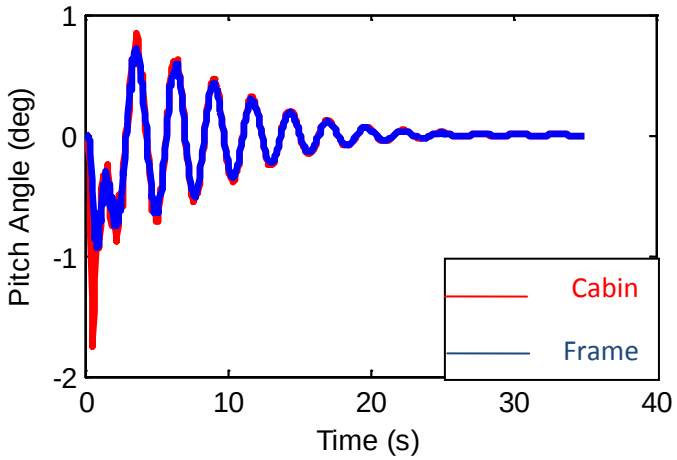

Figure 5.47 Cabin/Frame pitch angle-time comparison

Figure 5.47 shows that cabin and frame move synchronously with a 1° starting phase angle difference.

Table 5.6 Nodal displacements

Nodal Displacements		
Number of Nodes	Minimum/Maximum Values (m)	
nr1	Min	-0.148891
	Max	0.156935
nr2	Min	-0.188408
	Max	0.233701
nr5	Min	-0.131872
	Max	0.169297
nr6	Min	-0.180677
	Max	0.244856
nr7	Min	-0.136816
	Max	0.105287
nr9	Min	-0.173772
	Max	0.21496

Table 5.7 Nodal velocities

Nodal Velocities		
Number of Nodes	Minimum/Maximum Values (m/s)	
nr1	Min	-0.432285
	Max	0.559237
nr2	Min	-0.64226
	Max	0.921468

Table 5.8 Nodal accelerations

Nodal Accelerations		
Number of Nodes	Minimum/Maximum Values (m/s^2)	
nr1	Min	-2.10504
	Max	3.15398
nr2	Min	-3.64702
	Max	3.7755

Table 5.9 Dynamic characteristics of the vehicle

Crew Cabin Maximum Pitch Angle	-1.762°
Frame Maximum Pitch Angle	-0.9314°

5.3 Dynamic Responses of the Vehicle For Relative Sinusoidal Obstacle Transition

In this section bounce, roll, pitch and yaw reaction of both crew cabin and vehicle frame will be investigated. For calculating all intended phenomenon, nodal reactions "nr1 to nr9", which are used in previous sections, will also be used in this section.

Relative Sinusoidal Proving Ground will give ideas about the vehicle's reactions in all axis. Displacements in "x axis" according to ANSYS coordinate system will give the "yaw" response of the vehicle. We will start to check the responses with the bounce motion of the driver, commander and passenger in "y axis".

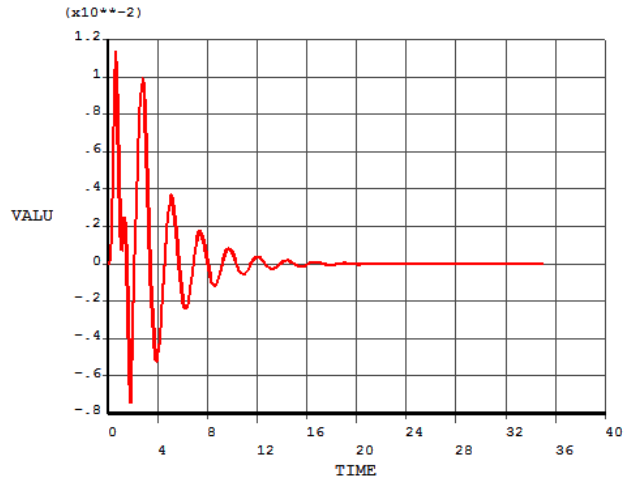

Figure 5.48 nr1 displacement-time graph

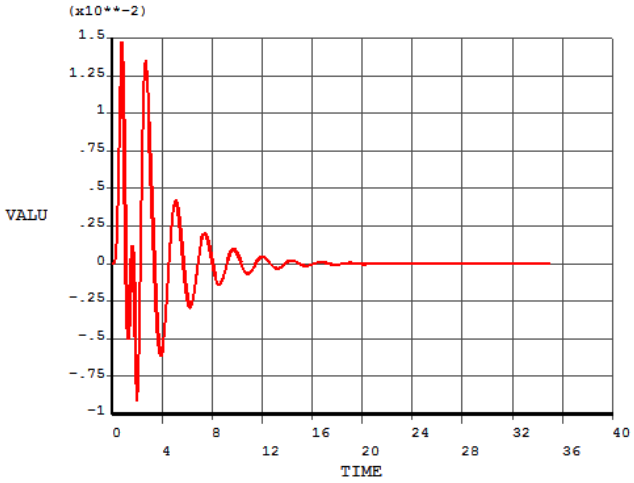

Figure 5.49 nr2 displacement-time graph

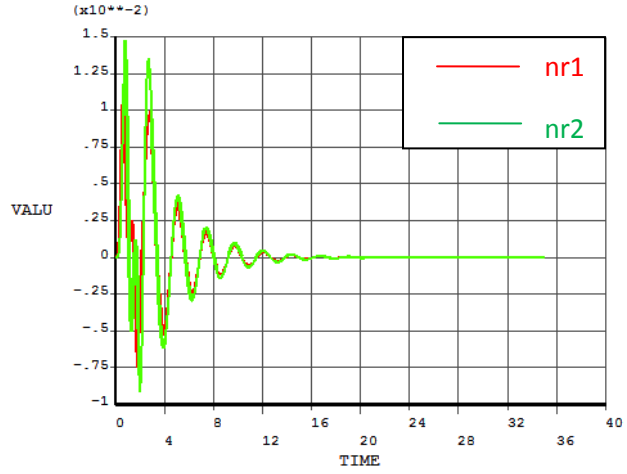

Figure 5.50 nr1/nr2 displacement-time comparison

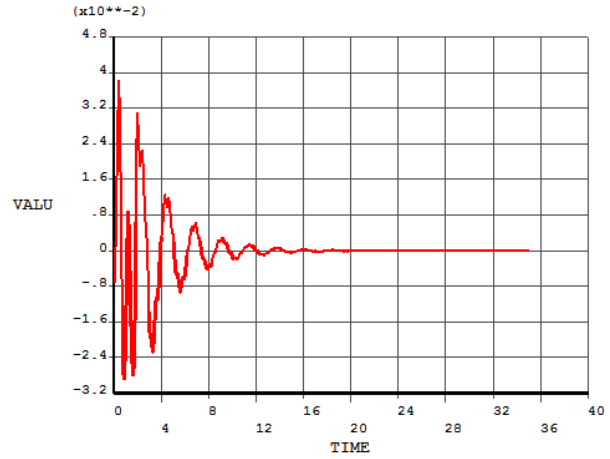

Figure 5.51 nr1 velocity-time graph

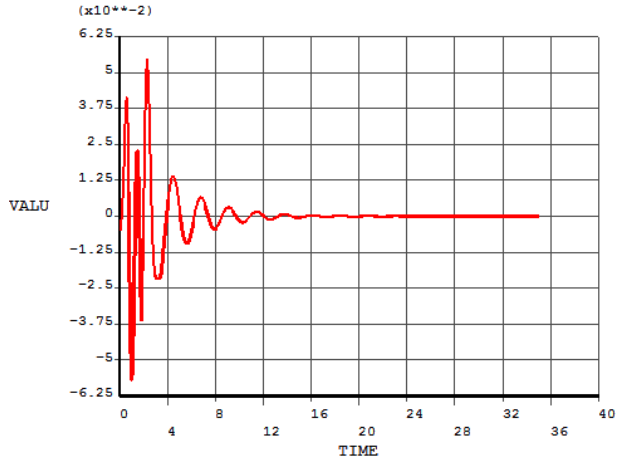

Figure 5.52 nr2 velocity-time graph

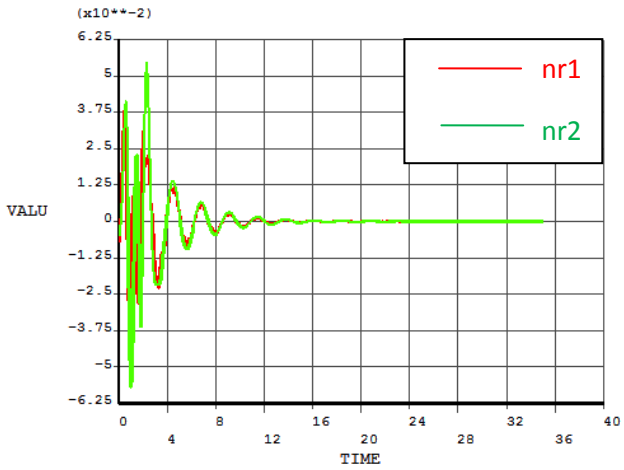

Figure 5.53 nr1/nr2 velocity-time comparison

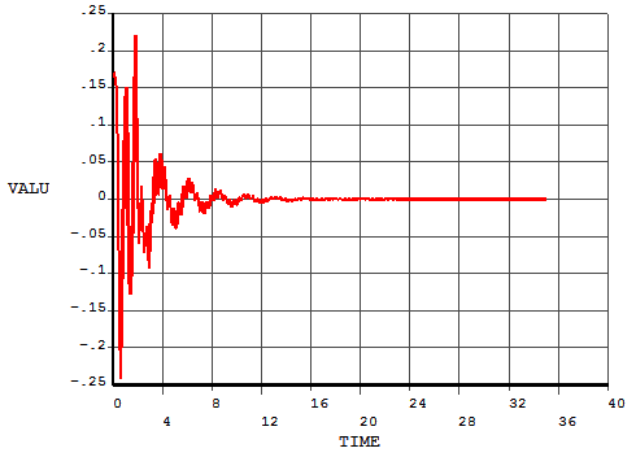

Figure 5.54 nr1 acceleration-time graph

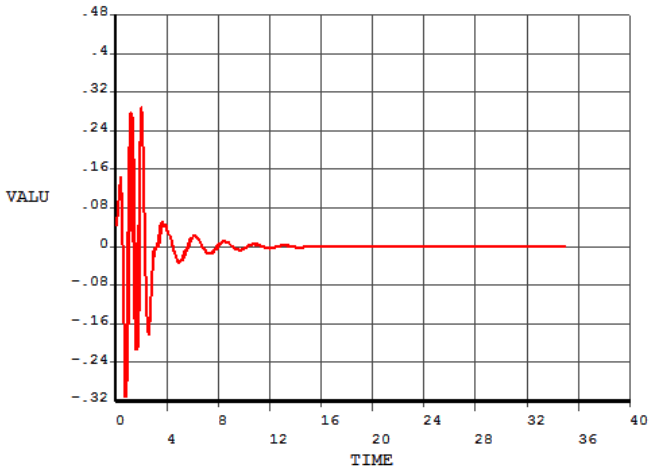

Figure 5.55 nr2 acceleration-time graph

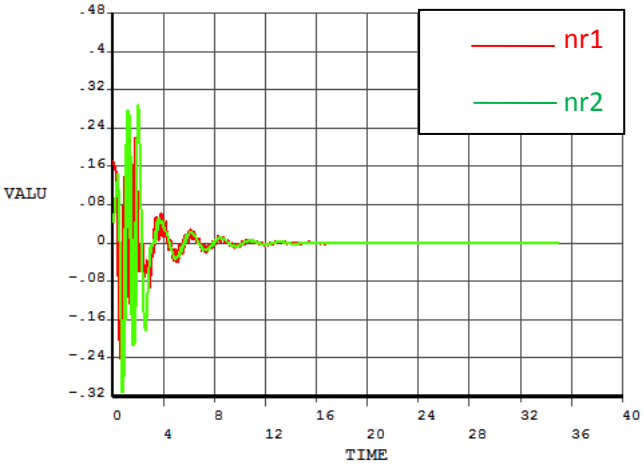

Figure 5.56 nr1/nr2 acceleration-time comparison

Above figures between Figure 5.48 and Figure 5.56 shows us the bounce motions of crew cabin and passenger at driver side. They both move on the same phase angle with different amplitudes like the other proving ground road conditions. Acceleration graphics show that passenger move smoother than the crew cabin, so we can comment that spring-damper elements damp the road excitations a few more than the cabin elements.

Responses belongs to commander side will be checked, the results will give the roll characteristic of the crew cabin.

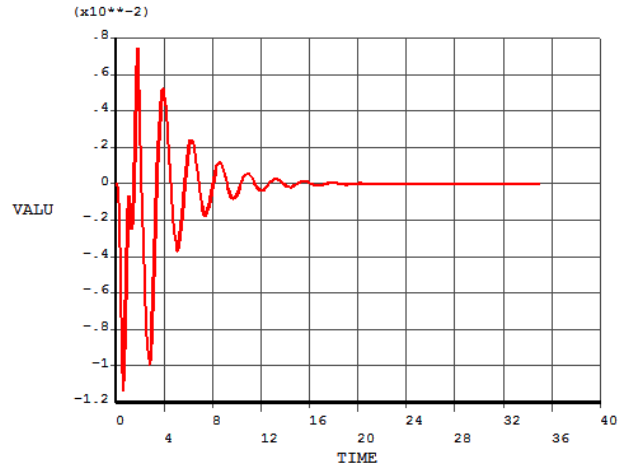

Figure 5.57 nr3 displacement-time graph

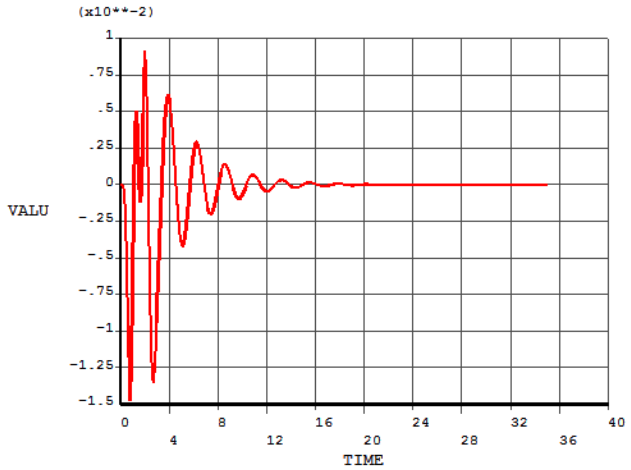

Figure 5.58 nr4 displacement-time graph

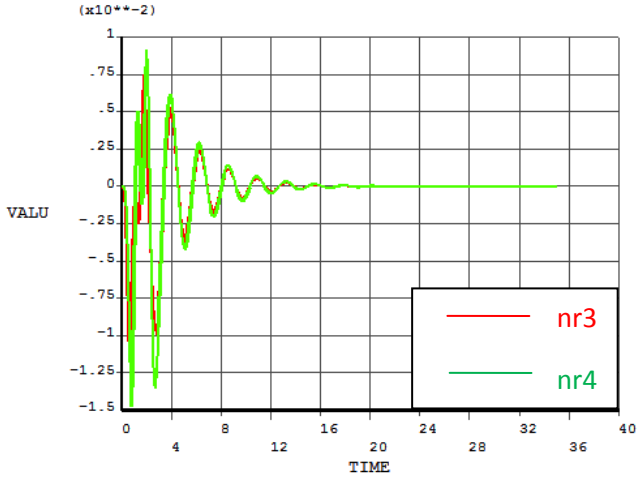

Figure 5.59 nr3/nr4 displacement-time comparison

Figure 5.59 shows the bounce motions of commander side. However they start moving in different phase angle, than the motion continues synchronously. Comparison between nr1 and nr3 will give the roll characteristic of the crew cabin.

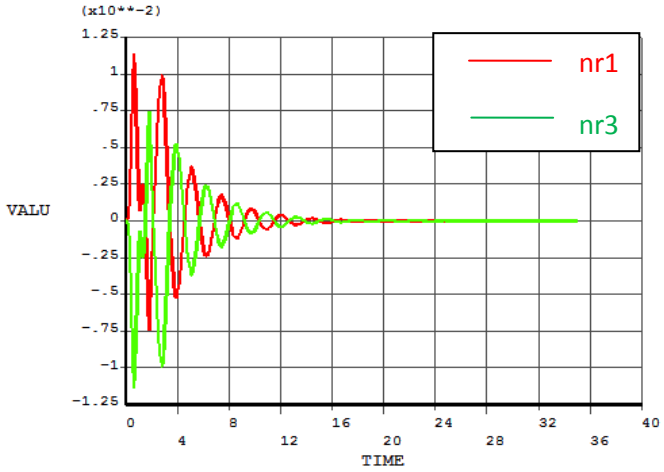

Figure 5.60 nr1/nr3 displacement-time comparison

Figure 5.60 shows than the roll motion occurs on the cabin. The amplitude of the motion will be calculated according to the parameters and formula given in Figure 5.15.

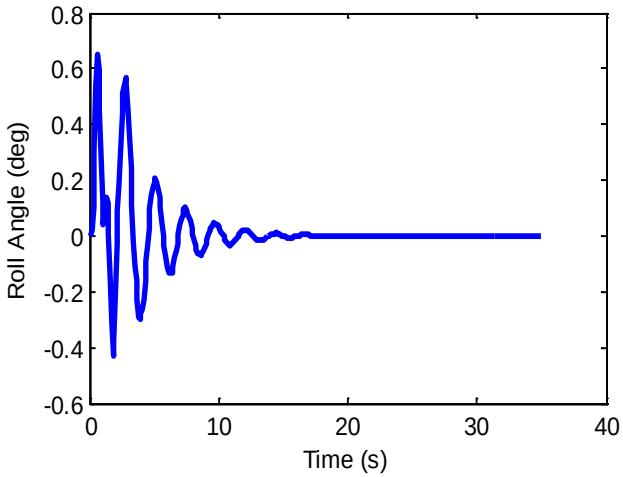

Figure 5.61 Cabin roll angle-time graph

As it is seen on Figure 5.61, cabin move with a maximum 0.65° roll angle, which corresponds a 3.9mm difference.

Passenger nodal reactions located on the second raw of the cabin will be figured.

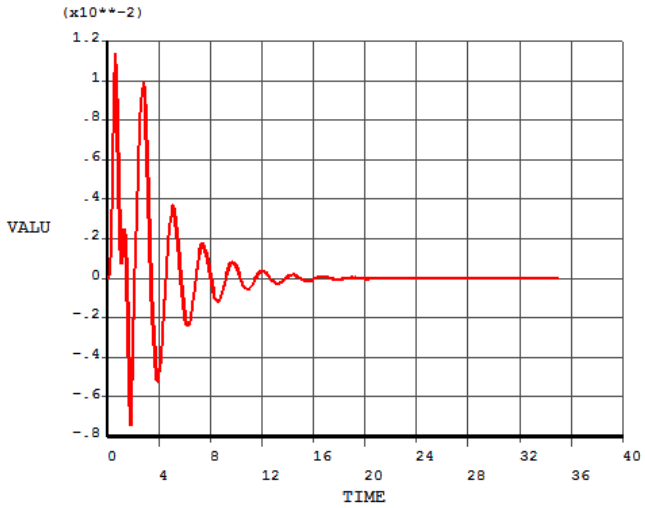

Figure 5.62 nr5 displacement-time graph

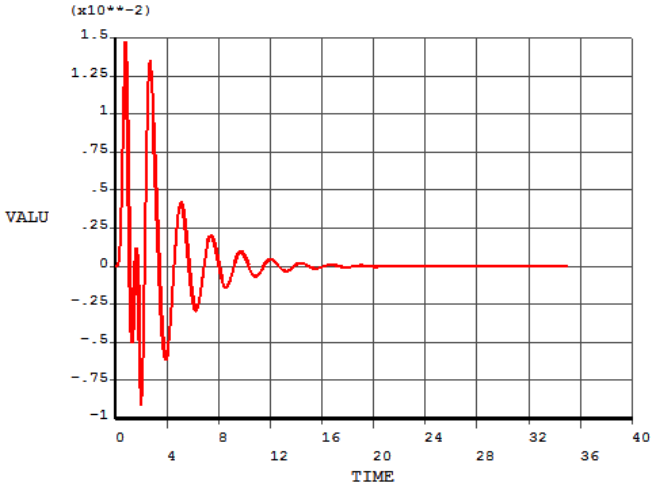

Figure 5.63 nr6 displacement-time graph

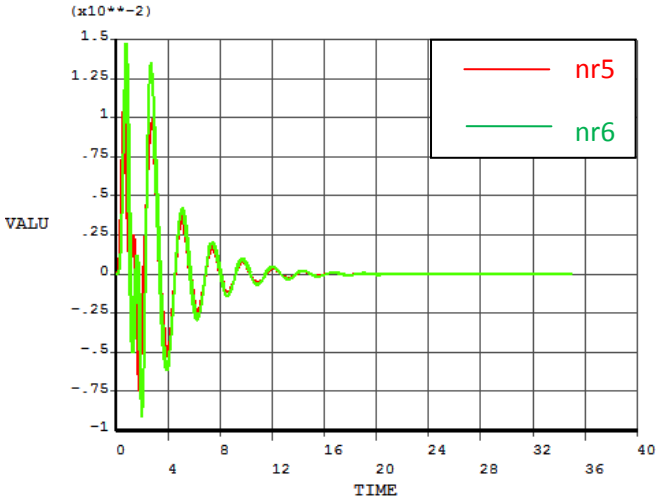

Figure 5.64 nr5/nr6 displacement-time comparison

Figure 5.64 shows that second raw bounce motions are nearly the same as first raw bounce motions. Comparison between nr1 and nr5 will give the pitch characteristic of the cabin. Below Figure 5.65 shows us no pitch motion occurs on crew cabin.

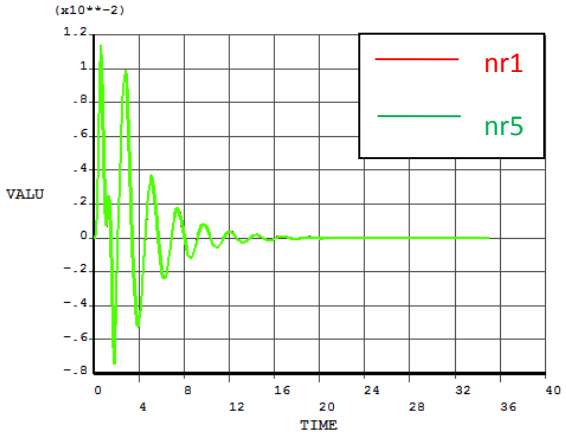

Figure 5.65 nr1/nr5 displacement-time comparison

Nodal reaction of the nodes nr7, nr8 and nr9 will be presented respectively in order to check the frame behaviour according to sinusoidal road excitations.

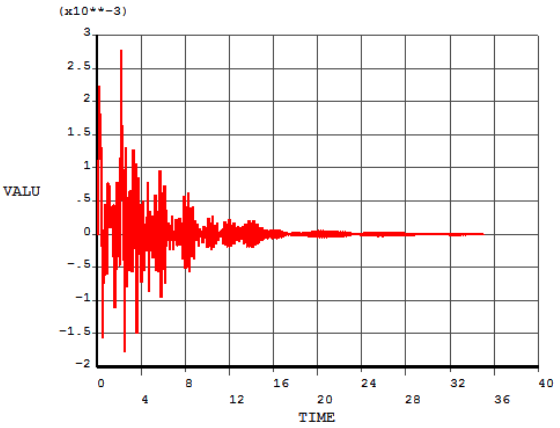

Figure 5.66 nr7 displacement-time graph

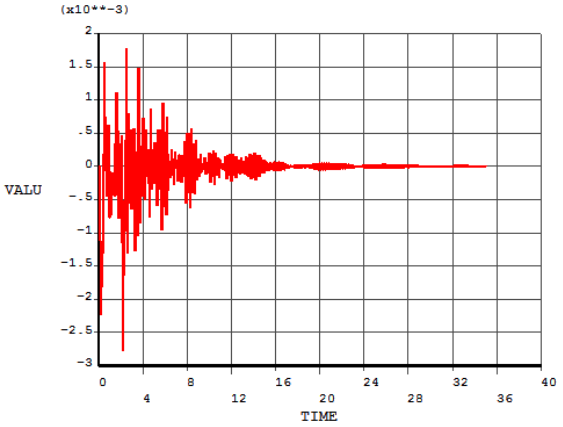

Figure 5.67 nr8 displacement-time graph

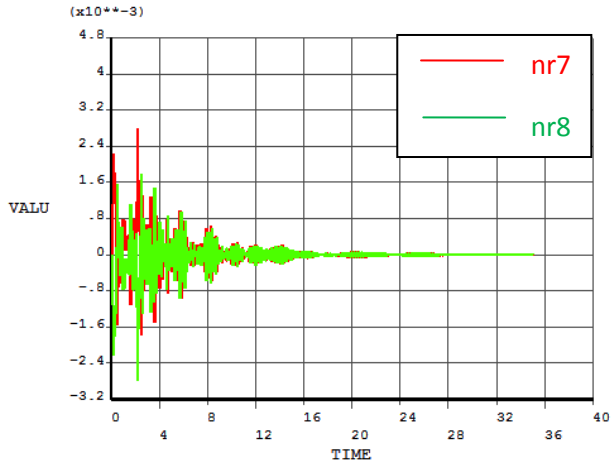

Figure 5.68 nr7/nr8 displacement-time comparison

Above figures shows that frame responses vibratory as a result of excitations. Graphics between Figure 5.48 and Figure 5.68 illustrate cabin-spring elements function successfully in order to damp the excitations, so a safe ride is supplied on the cabin side. Roll characteristic of the frame will be calculated by using Figure 5.69 via using the calculation method given in Figure 5.24.

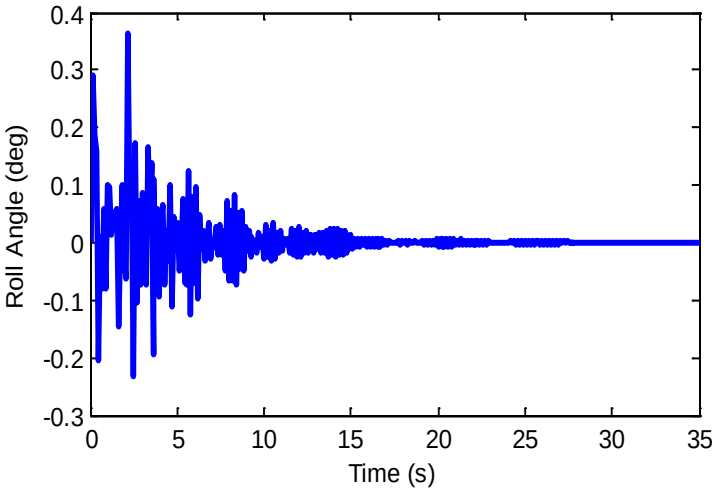

Figure 5.69 Frame roll angle-time graph

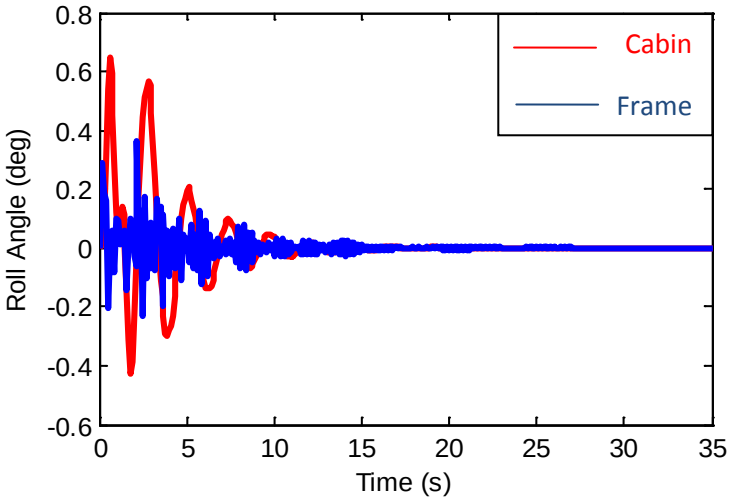

Figure 5.70 Cabin/Frame roll angle-time comparison

Figure 5.70 proves the function of the spring-damper elements between cabin-frame connection. They damp the excitations smoothly, so the handling will be under driver's control.

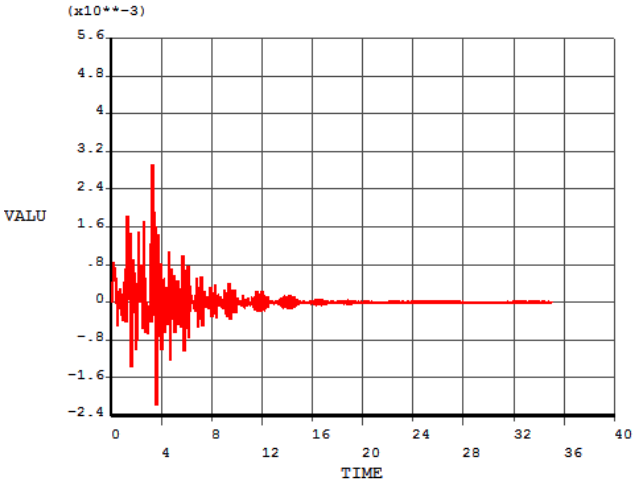

Figure 5.71 nr9 displacement-time graph

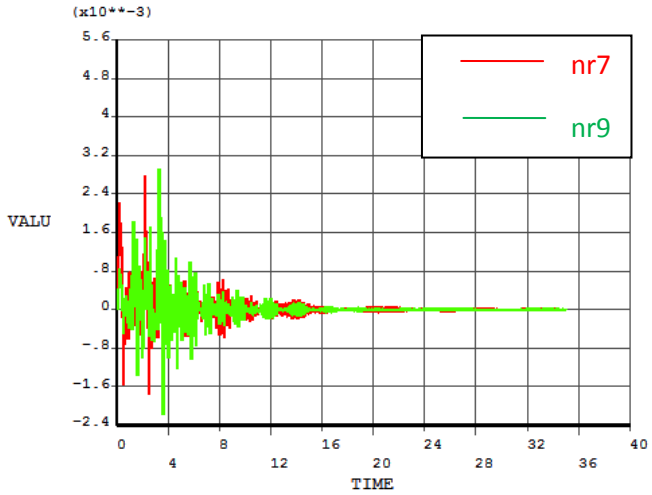

Figure 5.72 nr7/nr9 displacement-time comparison

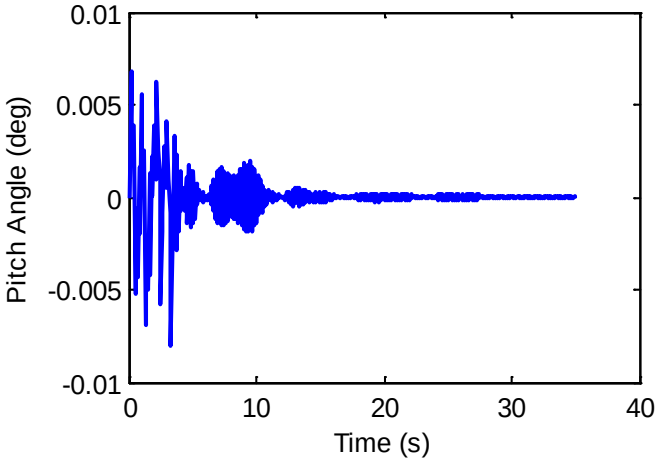

Figure 5.73 Frame pitch angle-time graph

However, frame is seen to have vibratory motion, maximum pitch angle is 0.0067°. In order to check the yaw response of the frame, displacements of nr7 and nr9 in "x axis" will be checked.

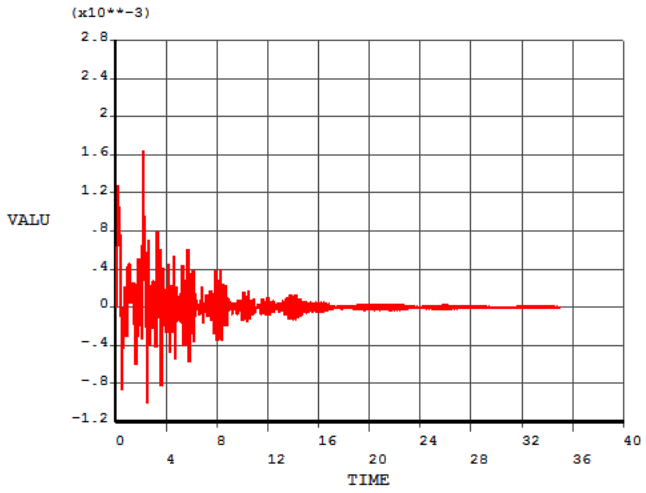

Figure 5.74 nr7 displacement in x axis-time graph

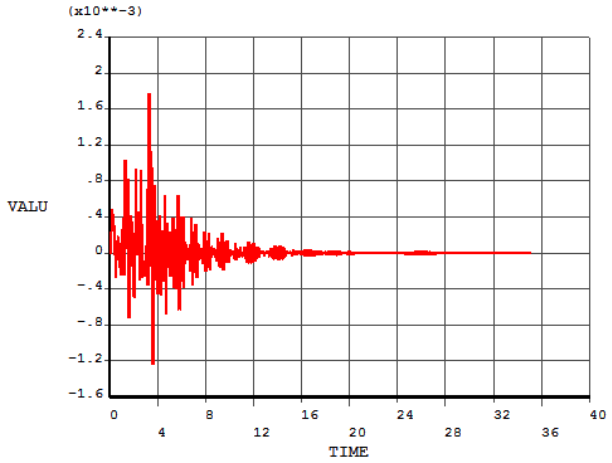

Figure 5.75 nr9 displacement in x axis-time graph

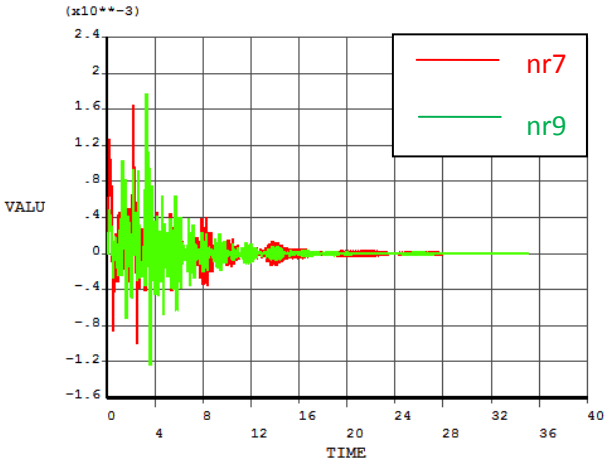

Figure 5.76 nr7-nr9 displacement in x axis-time comparison

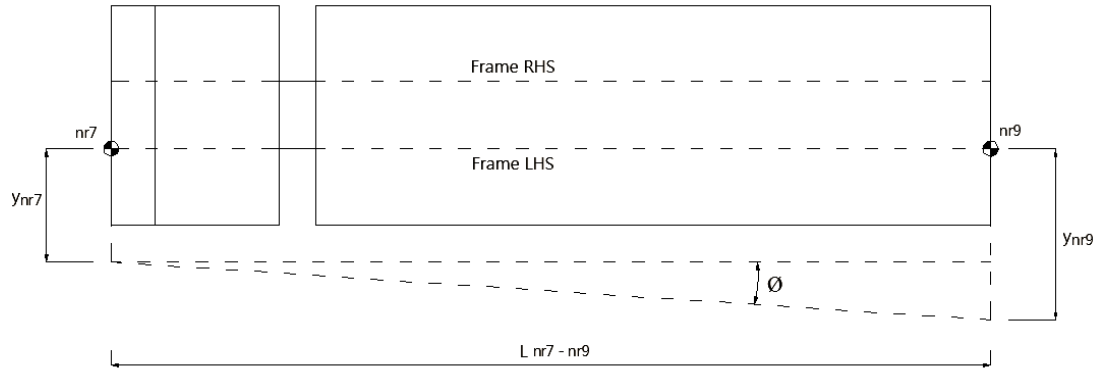

Figure 5.77 Top view of the vehicle, frame yaw parameters

$$\emptyset = tan^{-1}\left(\frac{x_{nr7}-x_{nr9}}{L_{nr7-nr9}}\right) \tag{5.5}$$

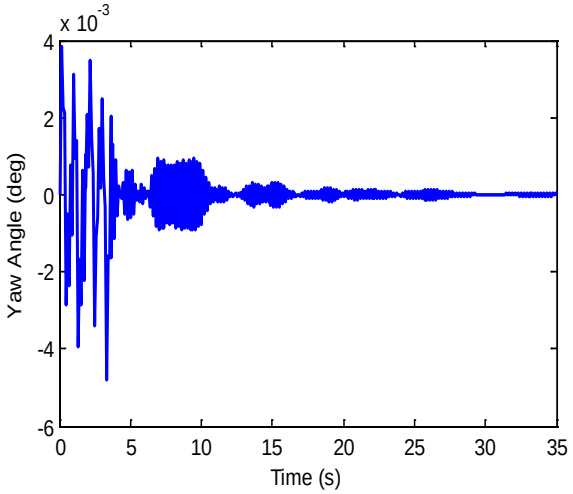

Figure 5.78 Frame yaw angle-time graph

As shown in Figure 5.78, maximum yaw angle of the frame is -0.004792°, that will show us yaw motion of the frame is nearly negligible. Double wishbone independent primary suspension seems really compatible to the sinusoidal road excitations.

Table 5.10 Nodal displacements

Nodal Displacements		
Number of Nodes	Minimum/Maximum Values (m)	
nr1	Min	-0.00745661
	Max	0.0113649
nr2	Min	-0.0091509
	Max	0.0147447
nr3	Min	-0.011366
	Max	0.00745603
nr4	Min	-0.0147465
	Max	0.00915043
nr5	Min	-0.00745398
	Max	0.01136
nr6	Min	-0.00914765
	Max	0.0147415
nr7	Min	-0.00176729
	Max	0.0027758
nr8	Min	-0.00277438
	Max	0.00176826
nr9	Min	-0.00218184
	Max	0.0029192

Table 5.11 Nodal velocities

Nodal Velocities		
Number of Nodes	Minimum/Maximum Values (m/s)	
nr1	Min	-0.0289079
	Max	0.0381938
nr2	Min	-0.0569278
	Max	0.0545539

Table 5.12 Nodal accelerations

Nodal Accelerations		
Number of Nodes	Minimum/Maximum Values (m/s^2)	
nr1	Min	-0.240745
	Max	0.220503
nr2	Min	-0.311528
	Max	0.287313

Table 5.13 Dynamic characteristics of the vehicle

Crew Cabin Maximum Roll Angle	0.6512°
Frame Maximum Roll Angle	0.3634°
Frame Maximum Pitch Angle	-0.008037°
Frame Maximum Yaw Angle	-0.004792°

CHAPTER SIX
RESULTS AND DISCUSSION

6.1 Evaluation of Dynamic Responses

In this study, different road excitations are applied as inputs to the multi-body dynamics model of the vehicle that is generated by initial calculations. Applied road excitations are specified, precisely in order to present the vehicle dynamic characteristics for bounce, roll, pitch and yaw cases. The results are examined respectively, maximum nodal values are displayed below, also the motion values of the driver are demonstrated.

6.1.1 Case 1 - Single Wheel Obstacle Transition

Single wheel obstacle transition case values are demonstrated in Table 6.1.

Table 6.1 Results for single wheel obstacle transition

Dynamic Response	No of Node	Max Value
Nodal displacement (maximum bounce)	nr6	0.175878 m
Driver seat maximum nodal displacement	nr2	0.174299 m
Driver seat maximum velocity	nr2	0.53772 m/s
Driver seat maximum acceleration	nr2	1.87854 m/s^2

6.1.2 Case 2 - All Wheel Obstacle Transition

All wheel obstacle transition case values are demonstrated in Table 6.2.

Table 6.2 Results for all wheel obstacle transition

Dynamic Response	No of Node	Max Value
Nodal displacement (maximum bounce)	nr6	0.244856 m
Driver seat maximum nodal displacement	nr2	0.233701 m
Driver seat maximum velocity	nr2	0.921468 m/s
Driver seat maximum acceleration	nr2	3.7755 m/s^2

6.1.3 Case 3 - Relative Sinusoidal Wheel Obstacle Transition

Relative sinusoidal wheel obstacle transition case values are demonstrated in Table 6.3.

Table 6.3 Results for relative sinusoidal wheel obstacle transition

Dynamic Response	No of Node	Max Value
Nodal displacement (maximum bounce)	nr4 ~ nr6	0.0147465 m
Driver seat maximum nodal displacement	nr2	0.0147447 m
Driver seat maximum velocity	nr2	0.0569278 m/s
Driver seat maximum acceleration	nr2	0.311528 m/s^2

For all proving ground conditions maximum bounce occurs in nr6 which is a passenger seat node in second row of the crew cabin. This is an expected situation because, it is well known that displacements increase through the back side of a vehicle. So this also shows us that, the finite element model is successful in displacement calculations.

Design targets can be expressed as; For nodal displacements, maximum displacement of any node should not exceed three times of the excitation amplitude. Maximum driver seat velocity should not be more than 1 m/s and the limit of the driver seat acceleration is half of gravitational acceleration. When the nodal results are checked, it is seen that values match with design targets.

However, the results demonstrate us vehicle is satisfactory from handling, riding and ride safety point of views, also subjective evaluations has to be performed in order to evaluate the effect of the system on the human body.

CHAPTER SEVEN
CONCLUSION

In this thesis, dynamic analysis of an eight-wheeled tactical vehicle, of which spring-damper element coefficients and constructive dimensions are specified, is presented. 3D finite element (FE) model of the vehicle is created in ANSYS. Suspension system is identified as a double wishbone independent suspension system, while secondary suspension system is simulated by locating existing mass (crew cabin) on four units of spring-damper couples.

Three different road excitations are modeled by MATLAB, then they are converted to ANSYS parametric design language by using Visual Basic.

Dynamic responses such as displacement, velocity and acceleration are obtained in selected nodes of the FE model. The responses of pitch, roll, yaw and bounce motions are extracted from these dynamic responses of the vehicle. Suitability of the cabin suspension system is evaluated by pitch, roll, yaw and bounce motions of the vehicle.

In this thesis, dynamic analysis of the vehicle is theoretically studied. Dynamic measurements can be performed to verify the FE model. Then, the corrections can be done according to the measurements if necessary.

REFERENCES

Daudpoto, D., Hussain, I.,& Memon, A. A. (2012). Introducing dual suspension system in road vehicles. *Mehran University Research Journal of Enginnering & Technology, 32,* 1-6.

Dixon, J. C. (2009).*Suspension geometry and computation,* John Wiley & Sons , Ltd.

Dowds, P.,& O'Dwyer, A. (2005). Modelling and control of a suspension system for vehicle applications. *Proceedings of the 4th Wismarer Automatisierungs Symposium,* Wismar, Germany.

Els, P. S. (2005). The applicability of ride comfort standarts to off-road vehicles. *Journal of Terramechanic, 42,* 47-64.

Els, P. S., Theron, N. J., Uys, P. E.,& Thoresson M. J. (2007). The ride comfort vs handling compromise for off-road vehicles. *Journal of Terramechanic, 44,* 303-317.

Hussain, I. (2012). *Multiple model based estimation of wheel-rail contact conditions.* Ph.D. Thesis, University of Salford. UK.

Jagirdar, V. V., Dadar, M. S.,& Sulakhe, V. P. (2010). Wishbone structure for front independent suspension of a military truck, *DESIDOC, Defence Science Journal, 60,* 178-183.

Maddaiah, K. C., Ratnam, D. V., Kumar, K. N., Kumar A. S., Yesu, A.,& Kumar, V. R. (2013). Design and analysis of automated truck cabin suspension system. *International Journal of Engineering Sciences & Research Technology, 34.*

Maurice, J. P.,& Vandenhoudt, J. (2013). Compromise between primary and secondary suspension. *Industry Vehicle Dynamics,* ATZ 0010000, 112.

Sanyal, A. K. (2004). *Dynamics and control of multibody systems in central gravity.* Ph.D. Thesis, University of Michigan. USA.

Sujatha, C., & Tejesu, P. (2002). Heavy vehicle dynamics-comparison between leaf spring and hydropneumatic suspensions, *Conference & Exposition on Structural Dynamics,* 2002 IMAC-XX-600 036.

Vaculin, O.,& Valasek, M. (2005). Influence of controlled suspension on truck stability. Multibody Dynamics, *ECCOMAS Thematic Conference,* Spain.

Zehsaz, M., Vakili-Tahami, F., Fasihi, A.,& Majidi Jirandi, A. A. (2012). Sensitivity of ride comfort to suspension characteristics of an off-road vehicle under road excitation. *International Journal of Emerging Technology and Advanced Engineering,* ISSN 2250-2459, 2, 5.

Valero, B., Amirouche, F., Mayton, A.,& Jobes, C. (2007). Comparison of passive seat suspension with different configuration of seat pads and active seat suspension, *SAE Technical Paper,* 312-996-3601.

APPENDICES

1 Matlab Codes For Mathematical Formulation of Relative Sinusoidal Road Profile

1.1 Sinusoidal Road Profile For Left Wheel

```
clc,clear
dt=0.1;ta=0.4;
t=0:dt:5*ta;
w=2*pi/(2*ta)
y=0.3*sin(w*t);
plot(t,y,'r')
fl=fopen('D:\MSc\Thesis\0_Ths\Track\track_lt_dt01.txt','w');
fprintf(fl,'%6.3f\r\n',y);fclose(fl);
hold on
```

1.2 Sinusoidal Road Profile For Right Wheel

```
clc,clear
dt=0.1;ta=0.4;
t=0:dt:5*ta;
w=2*pi/(2*ta)
y=0.3*cos(w*t+pi/2);
plot(t,y)
fl=fopen('D:\MSc\Thesis\0_Ths\Track\track_rt_dt01.txt','w');
fprintf(fl,'%6.3f\r\n',y);fclose(fl);
```

1.2 Matlab Code For Vehicle Modal Responses

```
p0                      %eigenvalue of the system
x=abs(real(p0));
```

```
y=abs(imag(p0));
w0=sqrt(x^2+y^2);
ksi=x/w0                %damping of the system
t0=2*pi/w0              %period of the system
f0=1/t0                 %frequency of the system
dt=t0/20                %time increment of the system
tson=t0/ksi             %infinite time of the system
```

1.3 Matlab Codes For Single Wheel Obstacle Transition

1.3.1 Base Excitation

```
time, 0.22
d,9,uy, 0.10
solve
time, 0.44
d,29,uy, 0.10
solve
time, 0.83
d,49,uy, 0.10
solve
time, 1.05
d,69,uy, 0.10
solve
time, 1.27
d,9,uy, 0
solve
time, 1.49
d,29,uy, 0
solve
time, 1.88
d,49,uy, 0
```

```
solve
time, 2.1
d,69,uy, 0
solve
```

1.3.2 Crew Cabin Roll Angle

```
clc;clear;
h1=load('D:\MSc\Thesis\0_Ths\ths4_roll_calculation\PRVAR_nr1_115.txt')
t=h1(:,1);
ynr1=h1(:,2);
%plot(t,ynr1,'r')
h2=load('D:\MSc\Thesis\0_Ths\ths4_roll_calculation\PRVAR_nr3_117.txt')
%t=h2(:,1);
ynr3=h2(:,2);
%plot(t,ynr3,'b')
y=ynr1-ynr3;
L=2;
t2=y/L;
r=atan(t2);
cabinroll=r*180/pi;
plot(t,cabinroll,'b')
```

1.3.3 Crew Cabin Pitch Angle

```
clc;clear;
h1=load('D:\MSc\Thesis\0_Ths\ths4_roll_calculation\PRVAR_nr1_115.txt')
t=h1(:,1);
ynr1=h1(:,2);
h3=load('D:\MSc\Thesis\0_Ths\ths4_roll_calculation\PRVAR_nr5_119.txt')
ynr5=h3(:,2);
y=ynr1-ynr5;
```

```
L=1.045;
t2=y/L;
r=atan(t2);
cabinpitch=r*180/pi;
plot(t, cabinpitch,'b')
```

1.3.4 Frame Roll Angle

```
clc;clear;
h3=load('D:\MSc\Thesis\0_Ths\ths4_roll_calculation\frame\PRVAR_nr7_85.txt');
t=h3(:,1);
ynr7=h3(:,2);
h4=load('D:\MSc\Thesis\0_Ths\ths4_roll_calculation\frame\PRVAR_nr8_86.txt');
ynr8=h4(:,2);
yf=ynr7-ynr8;
Lf=0.875;
tf=yf/Lf;
tf=[tf'];
rf=atan(tf);
frameroll=rf*180/pi
plot(t, frameroll,'b')
```

1.4 Matlab Codes For All Wheel Obstacle Transition

1.4.1 Base Excitation

```
time, 0.22
d,9,uy, 0.10
d,19,uy, 0.10
solve
time, 0.44
d,29,uy, 0.10
```

```
d,39,uy, 0.10
solve
time, 0.83
d,49,uy, 0.10
d,59,uy, 0.10
solve
time, 1.05
d,69,uy, 0.10
d,79,uy, 0.10
solve
time, 1.27
d,9,uy, 0
d,19,uy, 0
solve
time, 1.49
d,29,uy, 0
d,39,uy, 0
solve
time, 1.88
d,49,uy, 0
d,59,uy, 0
solve
time, 2.1
d,69,uy, 0
d,79,uy, 0
solve
```

1.4.2 Crew Cabin Pitch Angle

```
clc;clear;
h5=load('D:\MSc\Thesis\0_Ths\ths5_roll_calculation\PRVAR_nr1_115.txt')
t=h5(:,1);
```

```
ynr1=h5(:,2);
h6=load('D:\MSc\Thesis\0_Ths\ths5_roll_calculation\PRVAR_nr5_119.txt')
ynr5=h6(:,2);
y=ynr1-ynr5;
L=1.045;
t2=y/L;
r=atan(t2);
cabinpitch=r*180/pi;
plot(t, cabinpitch,'r')
hold on
```

1.4.3 Frame Pitch Angle

```
clc;clear;
h7=load('D:\MSc\Thesis\0_Ths\ths5_roll_calculation\PRVAR_nr7_85.txt')
t=h7(:,1);
ynr7=h7(:,2);
h8=load('D:\MSc\Thesis\0_Ths\ths5_roll_calculation\PRVAR_nr9_125.txt')
ynr9=h8(:,2);
y=ynr7-ynr9;
L=11.795;  t2=y/L;
r=atan(t2);
framepitch=r*180/pi;
plot(t, framepitch,'b')
```

1.5 Matlab Codes For Relative Sinusoidal Obstacle Transition

1.5.1 Crew Cabin Roll Angle

```
clc;clear;
h7=load('D:\MSc\Thesis\0_Ths\ths6_roll_pitch_calculation\PRVAR_nr1_115.txt')
t=h7(:,1);
```

```
ynr1=h7(:,2);
h8=load('D:\MSc\Thesis\0_Ths\ths6_roll_pitch_calculation\PRVAR_nr3_117.txt')
ynr3=h8(:,2);
y=ynr1-ynr3;
L=2;
t2=y/L;
r=atan(t2);
cabinroll=r*180/pi;
plot(t, cabinroll,'r')
hold on
```

1.5.2 Frame Roll Angle

```
h9=load('D:\MSc\Thesis\0_Ths\ths6_roll_pitch_calculation\PRVAR_nr7_85.txt')
t=h9(:,1);
ynr7=h9(:,2);
h9=load('D:\MSc\Thesis\0_Ths\ths6_roll_pitch_calculation\PRVAR_nr8_86.txt')
ynr8=h9(:,2);
y=ynr7-ynr8;
L=0.875;
t2=y/L;
r=atan(t2);
frameroll=r*180/pi;
plot(t, frameroll,'b')
```

1.5.3 Frame Pitch Angle

```
clc;clear;
h9=load('D:\MSc\Thesis\0_Ths\ths6_roll_pitch_calculation\PRVAR_nr7_85.txt')
t=h9(:,1);
ynr7=h9(:,2);
h10=load('D:\MSc\Thesis\0_Ths\ths6_roll_pitch_calculation\PRVAR_nr9_125.txt')
ynr9=h10(:,2);
```

```
y=ynr7-ynr9;
L=11.795;
t2=y/L;
r=atan(t2);
framepitch=r*180/pi;
plot(t, framepitch,'b')
```

1.5.4 Frame Yaw Angle

```
clc;clear;
h17=load('D:\MSc\Thesis\0_Ths\ths6_yaw_calculation\PRVAR_x85.txt')
t=h17(:,1);
ynr1=h17(:,2);
h18=load('D:\MSc\Thesis\0_Ths\ths6_yaw_calculation\PRVAR_x125.txt')
ynr3=h18(:,2);
y=ynr1-ynr3;
L=11.795;
t2=y/L;
r=atan(t2);
frameyaw=r*180/pi;
plot(t, frameyaw,'b')
```

1.6 Visual Basic Codes for Relative Sinusoidal Wheel Excitations

1.6.1 First Axle Left Wheel Excitation

```
Private Sub Form_Load()
fl0 = "D:\MSc\Thesis\0_Ths\Track\"
ns = 100000
ReDim y(ns) As Single
nfc = "9":
dt = 0.1
```

```
fl1 = "track_lt_dt01.txt"
fl2 = "left_1st_w_dt01.txt"
WindowState = 2: Cls
Open fl0 + fl1 For Input As 1: n = 0
10 If EOF(1) = -1 Then GoTo 15
   n = n + 1: Input #1, y(n): GoTo 10
15 Close #1: n = n + 1: y(n) = 0
  Open fl0 + fl2 For Output As 1: t = 0
  For i = 1 To n
  t = t + dt: Print #1, "time," + Str(t)
  Print #1, "d," + nfc + ",uy," + Str(y(i))
  Print #1, "solve"
  Next i
  Close #1: MsgBox (""): End
End Sub
```

1.6.2 Second Axle Left Wheel Excitation

```
Private Sub Form_Load()
fl0 = "D:\MSc\Thesis\0_Ths\Track\"
ns = 100000
ReDim y(ns) As Single
nfc = "29":
dt = 0.1
fl1 = "track_lt_dt01.txt"
fl2 = "left_2nd_w_dt01.txt"
WindowState = 2: Cls
Open fl0 + fl1 For Input As 1: n = 0
10 If EOF(1) = -1 Then GoTo 15
   n = n + 1: Input #1, y(n): GoTo 10
15 Close #1: n = n + 1: y(n) = 0
  Open fl0 + fl2 For Output As 1: t = 4 * dt
```

```
 For i = 1 To n + 4 * dt
 t = t + dt: Print #1, "time," + Str(t)
 Print #1, "d," + nfc + ",uy," + Str(y(i))
 Print #1, "solve"
 Next i
 Close #1: MsgBox (""): End
End Sub
```

1.6.3 Third Axle Left Wheel Excitation

```
Private Sub Form_Load()
fl0 = "D:\MSc\Thesis\0_Ths\Track\"
ns = 100000
ReDim y(ns) As Single
nfc = "49":
dt = 0.1
fl1 = "track_lt_dt01.txt"
fl2 = "left_3rd_w_dt01.txt"
WindowState = 2: Cls
Open fl0 + fl1 For Input As 1: n = 0
10 If EOF(1) = -1 Then GoTo 15
   n = n + 1: Input #1, y(n): GoTo 10
15 Close #1: n = n + 1: y(n) = 0
 Open fl0 + fl2 For Output As 1: t = dt * 11
 For i = 1 To n + dt * 11
 t = t + dt: Print #1, "time," + Str(t)
 Print #1, "d," + nfc + ",uy," + Str(y(i))
 Print #1, "solve"
 Next i
 Close #1: MsgBox (""): End
End Sub
```

1.6.4 Fourth Axle Left Wheel Excitation

```
Private Sub Form_Load()
fl0 = "D:\MSc\Thesis\0_Ths\Track\"
ns = 100000
ReDim y(ns) As Single
nfc = "69":
dt = 0.1
fl1 = "track_lt_dt01.txt"
fl2 = "left_4th_w_dt01.txt"
WindowState = 2: Cls
Open fl0 + fl1 For Input As 1: n = 0
10 If EOF(1) = -1 Then GoTo 15
   n = n + 1: Input #1, y(n): GoTo 10
15 Close #1: n = n + 1: y(n) = 0
  Open fl0 + fl2 For Output As 1: t = dt * 15
  For i = 1 To n + dt * 15
  t = t + dt: Print #1, "time," + Str(t)
  Print #1, "d," + nfc + ",uy," + Str(y(i))
  Print #1, "solve"
  Next i
  Close #1: MsgBox (""): End
End Sub
```

1.6.5 First Axle Right Wheel Excitation

```
Private Sub Form_Load()
fl0 = "D:\MSc\Thesis\0_Ths\Track\"
ns = 100000
ReDim y(ns) As Single
nfc = "19":
dt = 0.1
```

```
fl1 = "track_rt_dt01.txt"
fl2 = "right_1st_w_dt01.txt"
WindowState = 2: Cls
Open fl0 + fl1 For Input As 1: n = 0
10 If EOF(1) = -1 Then GoTo 15
   n = n + 1: Input #1, y(n): GoTo 10
15 Close #1: n = n + 1: y(n) = 0
  Open fl0 + fl2 For Output As 1: t = 0
  For i = 1 To n
  t = t + dt: Print #1, "time," + Str(t)
  Print #1, "d," + nfc + ",uy," + Str(y(i))
  Print #1, "solve"
  Next i
  Close #1: MsgBox (""): End
End Sub
```

1.6.6 Second Axle Right Wheel Excitation

```
Private Sub Form_Load()
fl0 = "D:\MSc\Thesis\0_Ths\Track\"
ns = 100000
ReDim y(ns) As Single
nfc = "39":
dt = 0.1
fl1 = "track_rt_dt01.txt"
fl2 = "right_2nd_w_dt01.txt"
WindowState = 2: Cls
Open fl0 + fl1 For Input As 1: n = 0
10 If EOF(1) = -1 Then GoTo 15
   n = n + 1: Input #1, y(n): GoTo 10
15 Close #1: n = n + 1: y(n) = 0
  Open fl0 + fl2 For Output As 1: t = dt * 4
```

```
 For i = 1 To n + dt * 4
 t = t + dt: Print #1, "time," + Str(t)
 Print #1, "d," + nfc + ",uy," + Str(y(i))
 Print #1, "solve"
 Next i
 Close #1: MsgBox (""): End
End Sub
```

1.6.7 Third Axle Right Wheel Excitation

```
Private Sub Form_Load()
fl0 = "D:\MSc\Thesis\0_Ths\Track\"
ns = 100000
ReDim y(ns) As Single
nfc = "59":
dt = 0.1
fl1 = "track_rt_dt01.txt"
fl2 = "right_3rd_w_dt01.txt"
WindowState = 2: Cls
Open fl0 + fl1 For Input As 1: n = 0
10 If EOF(1) = -1 Then GoTo 15
   n = n + 1: Input #1, y(n): GoTo 10
15 Close #1: n = n + 1: y(n) = 0
 Open fl0 + fl2 For Output As 1: t = dt * 11
 For i = 1 To n + dt * 11
 t = t + dt: Print #1, "time," + Str(t)
 Print #1, "d," + nfc + ",uy," + Str(y(i))
 Print #1, "solve"
 Next i
 Close #1: MsgBox (""): End
End Sub
```

1.6.8 Fourth Axle Right Wheel Excitation

```
Private Sub Form_Load()
fl0 = "D:\MSc\Thesis\0_Ths\Track\"
ns = 100000
ReDim y(ns) As Single
nfc = "79":
dt = 0.1
fl1 = "track_rt_dt01.txt"
fl2 = "right_4th_w_dt01.txt"
WindowState = 2: Cls
Open fl0 + fl1 For Input As 1: n = 0
10 If EOF(1) = -1 Then GoTo 15
   n = n + 1: Input #1, y(n): GoTo 10
15 Close #1: n = n + 1: y(n) = 0
  Open fl0 + fl2 For Output As 1: t = dt * 15
  For i = 1 To n + dt * 15
  t = t + dt: Print #1, "time," + Str(t)
  Print #1, "d," + nfc + ",uy," + Str(y(i))
  Print #1, "solve"
  Next i
  Close #1: MsgBox (""): End Sub
```